Analysis of seismic reflection data from the Northern Hispaniola margin: Implications for the recent evolution of the Northern Caribbean Plate boundary

Alana Oliveira de Sa, Sylvie Leroy, Elia d'Acremont, Sara Lafuerza, José Luis Granja-Bruña, Roberte Momplaisir, Dominique Boisson, Louise Watremez, Bladimir Moreno, Jordane Corbeau

Analysis of Seismic Reflection Data from the Northern Hispaniola Margin: Implications for the Recent Evolution of the Northern Caribbean Plate Boundary

Oliveira de Sá A.[1], Leroy S. [1], d'Acremont E.[1], Lafuerza S.[1], Granja-Buña J.L.[2], Momplaisir R. [3], Boisson D. [3], Watremez L.[4], Moreno B. [5], Corbeau J. [6]

1 Sorbonne Université, CNRS, ISTeP, Institut des Sciences de la Terre de Paris, France
2 Universidad Complutense, Madrid, Spain
3 Université d'Etat d'Haiti, Port-au-Prince, Haiti
4 Université de Lille, CNRS, Université Littoral Côte d'Opale, IRD, UMR 8187, Laboratoire d'Océanologie et de Géosciences, Lille, France
5 CENAIS, Santiago de Cuba, Cuba
6 IPGP Observatoire Martinique

Abstract

The northern margin of Hispaniola is characterised by an accretionary prism with morphological structures shaped by tectonic, hydrodynamics and sedimentary processes in a context of oblique convergence between the North American and Caribbean plates. The Haiti Seismic Investigation (HAITISIS) of the northern Caribbean plate boundary elucidates the relationships between fault-driven tectonic activity, seafloor morphology, and the effects of transpressional deformation. We evidence an E-W-trending spatial variation in deformation accommodation and sedimentary records along the accretionary prism. The distinct morpho-structural character of the seafloor and sedimentation patterns of the Eastern and Western domains of the northern Hispaniola margin originated during the Upper Miocene-Pliocene tectonic reorganisation of the northern Caribbean Plate boundary. This regional reorganisation is associated with the onset of the oblique collision of the Caribbean and North American Plates that carried Hispaniola to the transpressive plate boundary opposite the Bahamas Carbonate Platform. This tectonic process led to the formation of an accretionary prism and activated segments of the eastern strand of the Septentrional-Oriente Fault Zone (SOFZ), resulting in lateral sediment source displacements and influencing sedimentary infill and deformation patterns. A mass transport deposit (MTD) in the Eastern domain is believed to have formed during this period of tectonic instability. Differential compaction and remobilisation of recent seismic units caused by the MTD have affected the seafloor morphology of the Eastern domain. The MTD is absent in the Western domain, the canyons are found in the Eastern domain.

Our interpretation of the early Miocene onset of the SOFZ and its evolution differs from previous studies that assume continuous eastward propagation. Morphologic features such as lateral displacement of canyons provide a chronology for the development of strike-slip and thrust faults prior to initiation of the SOFZ and the formation of the current fault segments of the SOFZ. Additionally, the variations in fault density, cumulative displacement along strike-slip faults, the morphology of the Northern Hispaniola insular slope (including width and tectonic style), and the tilting of basin surfaces suggest that the underthrusting of the North American plate beneath the Caribbean plate has ceased at the transition between the studied eastern and western domains. This pattern may be attributed to the westward rheological transition of the North American plate's crust (from oceanic to continental) at the level of the Bahamas platform.

Highlights

The northern Hispaniola margin is associated with an E-W-trending lateral change of the oblique convergence accommodation.

New chronology for the initiation and evolution of the Septentrional-Oriente Fault Zone thanks to submarine geomorphology.

Upper Miocene-Pliocene reorganization in the Northern Caribbean boundary linked to collision and distinct crustal domains.

1. Introduction

Active tectonic margins, including transpressional (shear + compression) margins, represent a large proportion of continental margins (e.g. Uyeda et al. 1984). Their seafloor morphology is governed by climatic, sedimentary, and oceanographic processes similar to those of passive margins. However, at active margins, tectonic activity controls the morphology at local and regional scales (Emery, 1980). Indeed, tectonic folding, faulting, uplift, and subsidence have been shown to directly affect the location, alignment, and geometry of many geomorphological features of active margin (Harris and Whiteway, 2011; McAdoo et al., 2000; Micallef et al., 2014). Therefore, it is essential to characterize the influence of tectonic activity on the emplacement and evolution of sedimentary systems in this context. This phenomenon remains poorly explored and nevertheless provides keys to a better understanding of the geodynamic evolution of the margin.

The northern Hispaniola margin offers an invaluable opportunity to investigate the interaction between tectonic-related faulting and seafloor morphology in transpressional plate boundary setting (Figures 1 and 2). The Septentrional-Oriente Fault Zone (SOFZ) delineates the northern boundary of the Caribbean Plate, tracing a WNW-ESE trajectory along this margin (Figures 1 and 2) (Leroy et al., 2015; Oliveira de Sá et al., 2021). The transpressive movement of the Caribbean Plate relative to the North American Plate in this area results in strain partitioning with the Northern Hispaniola Deformed Belt (NHDB) accommodating compression and the SOFZ accommodating shear (Calais et al., 2016; Mann et al., 2002; Rodriguez-Zurrunero et al., 2020). Strike-slip and compressive deformation have led to a diverse range of tectonic structures, such as fold-and-thrusts, strike-slip and normal faults, and basins (Calais et al., 2016; Rodríguez-Zurrunero et al., 2020) that significantly shape sedimentary processes and seafloor morphology (Figure 2b). A comprehensive understanding of this partitioned deformation system necessitates an in-depth analysis of the current northern boundary of the Caribbean Plate and its geodynamic evolution, focusing on the characterization of seafloor morpho-structures and their development over time. These factors collectively yield insights into the mechanics and dynamics of this active tectonic system and its impact on regional tectonic structure.

This analysis can potentially enhance the comprehension of the mechanisms by which oblique convergence is accommodated at the lateral transition between an obliquely subducting plate boundary and a transform plate boundary. This investigation is situated within the context of the lateral transition between oceanic and continental lithosphere in the lower plate.

Our study characterizes the structural and geomorphological framework of the northern Hispaniola margin using seismic reflection data and geomorphological analysis of high-resolution bathymetry data acquired during the HAITISIS 1 and 2 oceanographic expeditions (Leroy, 2012; Leroy and Ellouz-Zimmermann, 2013). Our objective is to determine the influence of tectonically induced subsurface deformation on the seafloor morphology and sedimentary systems in a transpressional plate boundary context. We investigate the sedimentary features and large-scale submarine canyon network intersected by strike-slip faults along the northern Haitian margin. High-resolution bathymetry shows how the deflection of the canyons highlights the regional strike-slip tectonic signature and the recent initiation of the eastern SOFZ along the Haitian margin. Furthermore, we discuss the variability of

morphological features, predominantly tied to the tectonic settings. This comprehensive examination enhances our understanding of the complex tectonic processes in the context of oblique convergence, their influence on the sedimentary and morphological features over time, and the current geometry of the northern boundary of the Caribbean Plate.

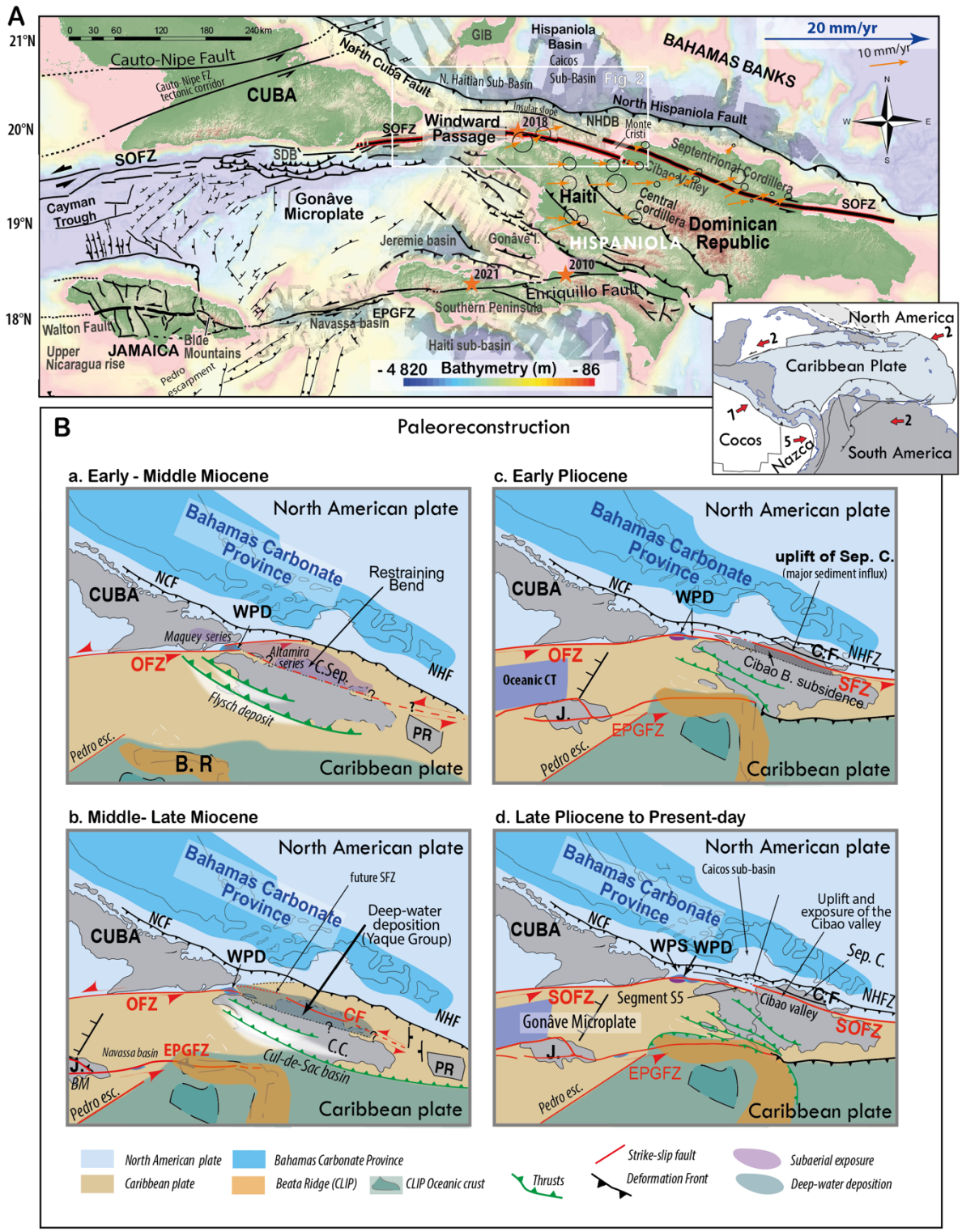

Figure 1. A) Tectonic map of the northern Caribbean plate boundary. NHDB: Northern Hispaniola Deformed Belt; SDB: Santiago Deformed Belt; SOFZ: Septentrional-Oriente Fault Zone, EPGFZ: Enriquillo Plantain Garden Fault Zone. The orange arrows indicate a GPS-derived velocity map expressed in the North American plate referenced frame (NAM08) with an ellipse error of 95% confidence (modified from Rodriguez-Zurrunero et al. 2020). White

frame is the Figure 2 area. Inset: Large-scale tectonic setting with arrows showing GPS-derived plate velocities in cm/y. The stars correspond to major earthquakes since 2010. B) Paleo-reconstruction/Tectonic setting of the northern boundary of the Caribbean plate from a. to d. Early-Middle Miocene to Late Pliocene – Present day, modified from Leroy et al. (2000), Calais & de Lépinay, 1995, Calais et al. (2016) and, Oliveira de Sá et al. (2021). See text for discussion. B.R: Beata Ridge; Pedro Esc.: Pedro Escarpment; NHF: North Hispaniola fault; NCF: North Cuba Fault; BM: Blue Mountains; J. Jamaica; C. Sept.: Septentrional Cordillera; PR: Porto Rico EPGFZ: Enriquillo-Plantain-Garden Fault Zone; OFZ: Oriente Fault Zone; CF: Camu Fault; SFZ: Septentrional Fault Zone; SOFZ: Septentrional Oriente Fault Zone; WPD: Windward Passage Deep; WPS: Windward Passage Sill.

2.1 Regional Tectonic Evolution and Current Setting

Since Eocene, the oblique collision between the Caribbean Plate and the Bahamas Carbonate Province has led to a southward migration of the North American-Caribbean Plate boundary by successive jumps of a major eastward propagating strike-slip fault system (Figure 1b; Mann et al., 1995; Leroy et al., 2000; Rojas-Agramonte et al., 2008; Iturralde-Vinent et al., 2016; Oliveira de Sá et al., 2021). In the Miocene, a major strike-slip fault, the Oriente Fault Zone (OFZ), ran along its southern Cuban coast, and then Cuba was already welded to the North American plate (Mann et al 1995, Leroy et al 2000) (Figure 1b – step a-b). During this time, the northern Hispaniola margin experienced an ongoing tectonic-driven reorganization related to the active oblique convergence (Calais et al., 2016; de Zoeten and Mann, 1999).

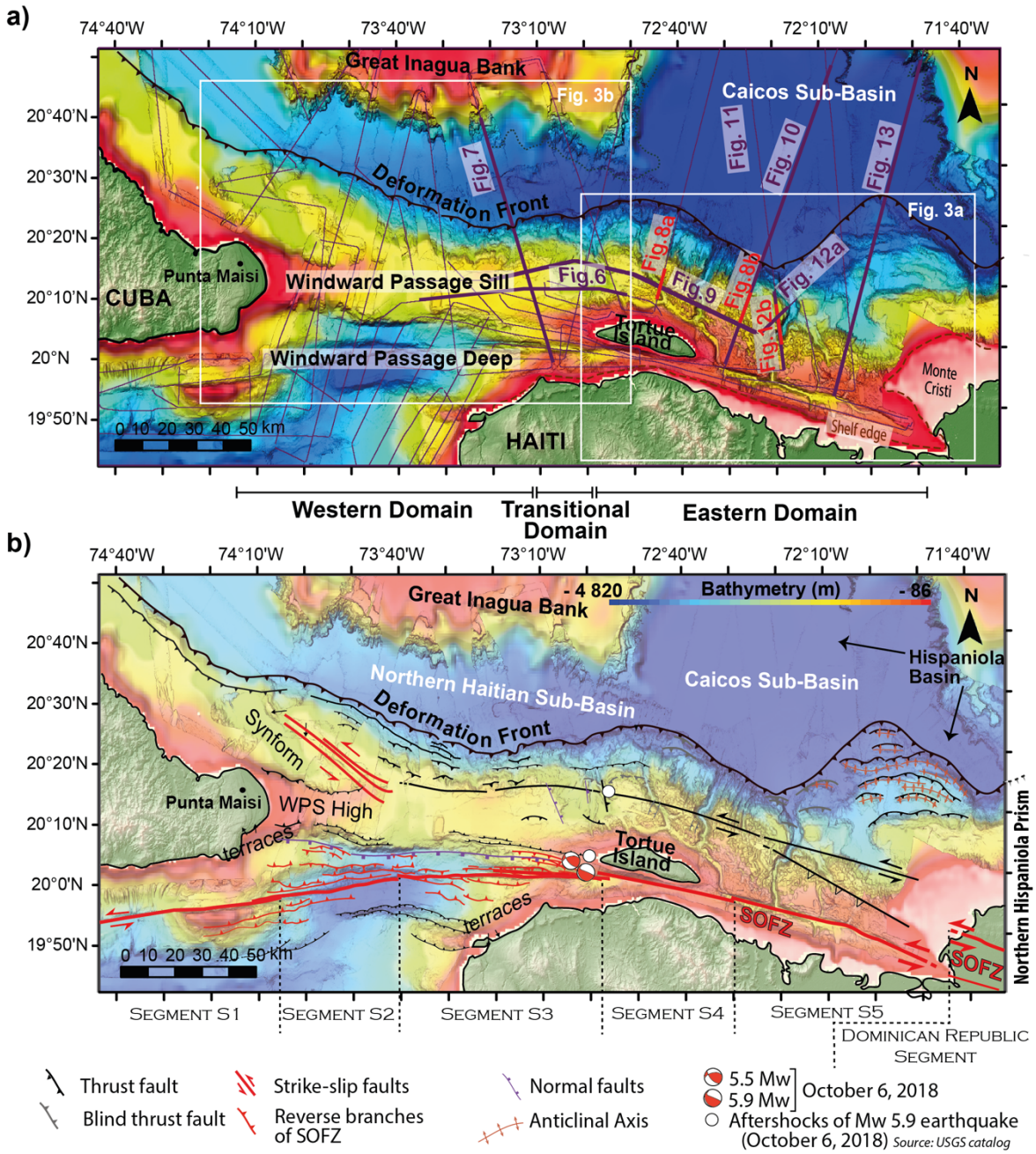

Figure 2: a) Bathymetric map showing the main morpho-structural domains of the Northern Haitian margin. Grey lines show the high-resolution 2D seismic reflection data used in the study. Violet lines indicate the location of the seismic lines used in this paper. White rectangles: detailed bathymetry maps shown in Figure 3. b) Structural map of the area. White dots: aftershocks of the Mw 5.9 earthquake of October 6 (2018). Source: USGS Catalog.

In the middle Miocene, the continuous transpressive stress resulted in the initiation of a strand of the future Septentrional Fault Zone (SFZ) and the development of a restraining bend along the northern margin of Hispaniola (Figure 1b – step a-b; Mann et al 1998; Leroy et al., 2000; Calais et al., 2016; Oliveira de Sá et al., 2021; Conrad et al 2024). As a result, geological formations in the Septentrional Cordillera experienced tilting, faulting, and folding (Figure 1a; de Zoeten and Mann, 1991, 1998, 1999; Erikson et al., 1998; McNeill et al 2013; Escuder-Viruete and Pérez, 2020). The eastward motion of the Caribbean Plate was slowed by its oblique collision with the Bahamas Carbonate Province (Figure 1b; Calais et al., 2016; Oliveira de Sá et al., 2021). The major strike-slip motion shifted progressively southward (Calais et al., 2016).

During the Pliocene, the OFZ splayed eastward, running across the Windward Passage Deep (WPD) into northern Hispaniola to form the present-day SOFZ, which is the current northern Caribbean Plate boundary (Figure 1b – step d; Oliveira de Sá et al., 2021; Calais and Mercier de Lépinay, 1995; Leroy et al., 2015). The WPD sedimentary cover allows Oliveira de Sá et al. (2021) to compute a ~80 km of left-lateral offset that occurred on the SOFZ segments since 5.4 ± 0.2 Ma (Figure 1b – step c-d; e.g., Oliveira de Sá et al., 2021).

Northern Hispaniola is also marked by a significant paleogeographic reorganization related to its late Pliocene oblique collision with the Bahamas Carbonate Province (Calais et al., 2016; Calais and Mercier De Lépinay, 1991; de Zoeten and Mann, 1999). Since the Pliocene, significant regional uplift resulted in the emergence of the Septentrional Cordillera (Calais et al., 2016; Erikson et al., 1998; McNeill et al 2013; Escuder-Viruete et al 2020). With the initiation of the SFZ, the present-day Septentrional Cordillera was transferred to the North American plate (Figure 1a; Calais et al., 2016; Calais and Mercier De Lépinay, 1995; Erikson et al., 1998; McNeill et al 2013; Leroy et al., 2015; Rodríguez-Zurrunero et al., 2019, 2020).

The Pliocene paleogeographic reorganization resulted in widespread strain distribution across the northern margin of Hispaniola. Currently, motion oblique to the plate boundary is mainly accommodated at a rate of 10–12 mm/yr by the SOFZ, which runs sub-parallel to the collision margin. While the deformation front of the Northern Hispaniola Prism accommodates motion normal to the boundary with an elastic strain at a rate of 1–3 mm/yr (Figure 2b; Benford et al., 2012; Calais et al., 2010; Dolan et al., 1998; Mann et al., 1995, 2002; Symithe et al., 2015).

2.2 Morpho-structural settings

The northern Haitian margin (Figures 2 and 3) extends 250 km from Windward Passage along the northern coast of Haiti, to the toe of the shallow Monte Cristi platform north of the Dominican Republic (Figures 1a and 2a). Depths along the margin range from 200 m to 4000 m. The margin is occupied by the Northern Hispaniola Prism (Figure 2b), which we interpret to be an accretionary prism defined by three domains (upper, middle, and lower prisms, Figure 4). The accretionary prism is also called the Northern Hispaniola Deformed Belt (NHDB, Figure 1a; Dillon et al., 1992, 1996; Rodríguez-Zurrunero et al., 2020). It consists of alternating broad anticline ridges and narrow troughs, trending roughly E-W, sub-parallel to the compressive deformation front (Figure 2b). This prism extends toward the east along the northern Dominican Republic (Rodriguez-Zurrunero et al., 2020) and to the west into the Old Bahamas Channel along the northern Cuban coast up to 77°W of longitude (Figure 1a; Oliveira de Sá et al., 2024).

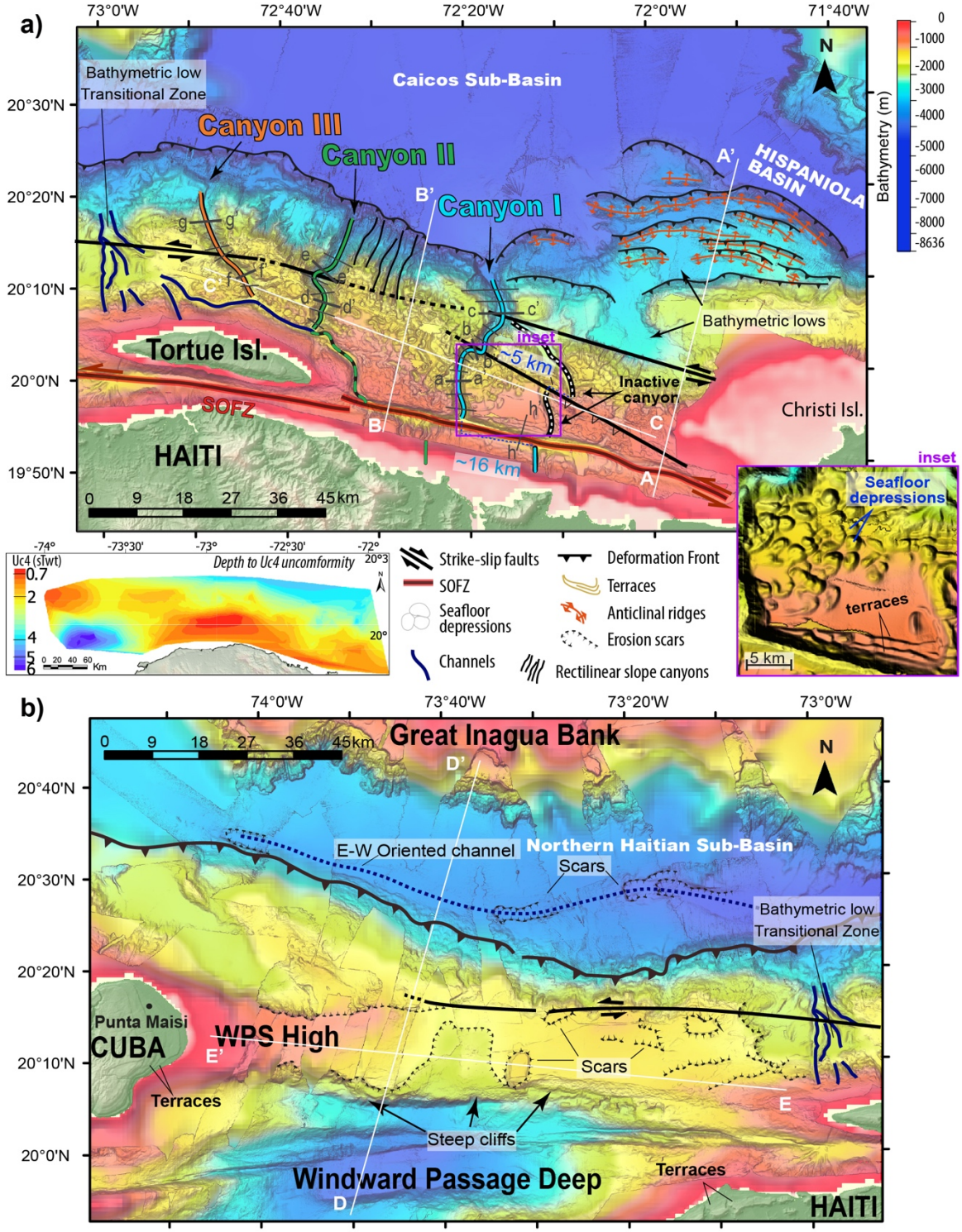

Figure 3. Bathymetric map with the interpretation of the principal seafloor geomorphological elements in the eastern (a) and Western domains (b). WPS High: Windward Passage Sill High. The Hispaniola basin is divided into two sub-basins: the Caicos sub-basin in the east and the Northern Haitian sub-basin, as proposed by Rodriguez-Zurrunero et al. 2020. Canyon I shows a 16 km shift, corresponding to 2 Ma of SOFZ activity (Leroy et al. 2015). See Authemayou et al. (2023) for terraces in Southern Cuba. White lines correspond to the cross-sections shown in Figure 4.

From 72°10'W to 72°50'W, a system of deeply incised north-south trending canyons stretches across the margin (Figure 3a). Approximately 2 Ma ago, the heads of these canyons were laterally deflected ~16 km ESE by the SOFZ (Figures 2b and 3a; Leroy et al., 2015). The seafloor in this region also displays several depressions (Figure 3a – inset).

Beyond 72°50', the edge of the Great Inagua Bank comes within 30 km of the Windward Passage Sill (WPS), and between them lies the narrow Northern Haitian sub-basin (Figure 2b). The depth of this basin is ~500 m shallower than that of Caicos sub-basin. In the Northern Haitian sub-basin, the E-W-trending basin floor gently inclines towards the east (Figure 3b). Large U-shaped scars occur between 72°50'W and 74°W on the floor of this channel, which are probably the result of slumping (Figure 3b) (Goreau, 1981), perhaps from sediments flowing towards the Caicos sub-basin (Figures 1, 2, and 3).

3. Data and Methodology

Multichannel seismic reflection and multibeam bathymetric data were collected during HAITISIS 1 and 2 (2012-2013) cruises onboard the R/V L'Atalante of the Flotte Océanographique Française (Leroy, 2012; Leroy and Ellouz-Zimmermann, 2013). Multibeam bathymetric data collected during the NORCARIBE geophysical cruise in 2013 aboard the Spanish R/V Sarmiento de Gamboa allows us to fill the gaps in our data coverage (Leroy et al. 2015; Rodríguez-Zurrunero et al., 2020). Our study focuses on the northern Hispaniola margin and the Winward Passage sill, where ~800 km of seismic reflection data were acquired (Figure 2a). Seismic reflection data were recorded using a fast and light seismic system comprised of two GI air guns source (2.46 L, 300 in3) and a 600 m long streamer with 24 traces operated at ~9.7 knots. The multichannel seismic reflection data were processed using classical steps, including CDP gathering (fold 6), binning at 25 m, detailed velocity analysis, stacking, and post-stack time migration. All the seismic reflection profiles presented were time-migrated with Seismic Unix®. Multibeam bathymetry data were acquired simultaneously with seismic profiles and gridded with a spacing of 50 m. The gridded bathymetry data was augmented with the GEBCO Digital Atlas (https://www.gebco.net/data_and_products/gebco_digital_atlas/) with an 800 m resolution to provide near-complete coverage (Figure 2a).

The processed seismic data were interpreted using Kingdom IHS Suite© software. Maps were plotted with ArcGIS® and Global Mapper® software. We used the seismic reflection dataset to identify sedimentary units and deformation styles and to infer the spatio-temporal evolution of the tectonic structures. Morphological analysis of the seafloor based on swath-bathymetric data was carried out to identify the surface signature of tectonic features (Figure 2). We identified faults by either sediment horizon offsets or by the fault plane seismic reflection in the seismic profiles.

4. Results

The northern Haitian margin exhibits two distinct domains: the Eastern domain extending from Christi Islands to Tortue Island (Figure 2a), and the Western domain located to the south of the Great Inagua Bank, including the area west of Tortue Island and Punta Maisi in Cuba (Figure 2b).

4.1 Morpho-structural Domains

In the Eastern domain (Figure 3a), seafloor morphology is very complex with deeply incised canyons beheaded and disconnected from the onshore sediment supplies by the lateral motion of the SOFZ at depth (section C-C' in Figures 3a and 4). The SOFZ is expressed at the

seafloor as a linear E-W trending channel off the Northern Haiti coast (Figures 3a and 4, section B-B' and inset b). The Eastern domain is also punctuated by various geomorphological features such as seafloor depressions (Figure 3a), terraces, gullies, and the anticlinal ridges of the lower prism (Figures 2 and 4). In addition, a buried MTD is observed. The upper, middle, and lower prisms occur in the eastern-most part of the Eastern domain. In the Western domain, only the upper and lower prims are observed (Figures 4; section B-B').

At 73°00'W to the west of Tortue Island, the extensive network of deeply incised canyons is absent, and the deformation front becomes more linear (Figure 3). Smaller, shallower canyons with relief of ~250 m are observed (Figure 3).

The Western domain encompasses the Windward Passage, situated west of Tortue Island (Figures 2 and 3b). In the area referred to as the WPS by Oliveira de Sá et al. (2021), the water depth gradually diminishes westward towards the Punta Maisi region (Figures 2, 3b, and 4, section E-E'). In the Western domain, the seafloor of the shelf between Cuba and Tortue Island shows no signs of canyon incisions or channels, no buried MTD, and none of the surface depressions visible in the seafloor of the Eastern domain. The seafloor is essentially flat but with some irregularities, such as large erosion scars, some of which create relief exceeding 300 m (WPS High west of section E-E' in Figure 4). Unlike longitudinal sections, cross-sections show a relatively flat seafloor that dips ~3.0° towards the North Haitian sub-basin near its northern edge and ~1.5° towards the WPD near its southern edge (Figure 4, section D-D'). This domain is bound by prominent cliffs along the northern and southern edges, particularly adjacent to the WPD (showing about 26° of dip, see Figures 3b and 4, section D-D'). The Northern Haitian sub-basin is very narrow, confined between the WPS and the Great Inagua Bank, and its floor shows a reverse dip towards the south (Figure 4, section D-D').

4.2 Submarine Canyons and Channels

In the Eastern domain, the SOFZ is marked by a deep, narrow channel in the southern-most margin near the Haitian shore. Here, five large terraces with depths ~1100m, ~1030 m, ~930 m, ~900 m, and ~875m form the northern wall of the fault channel (Figure 3 inset; section h-h' and inset b in Figure 4). In the Western domain, the SOFZ is characterized by a shallower, broader valley running between the Haitian shore and the southern shore of Tortue Island. The northern wall of Haiti is formed by two large terraces onshore (Figure 3 b).

Submarine canyons are present only in the Eastern domain (Figure 3a). The 3 largest canyons in the area (labelled I to III in Figures 3a and 4) trend north-south from the near-shore to the deformation front at the southern edge of the Caicos sub-basin, reaching depths of approximately ~4000 m (Figure 4, section B-B').

The head of Canyon I, east of Tortue Island, is located at the SOFZ channel, which is up to 1500 m deep (Figure 3a). The total length of this U-shaped canyon is ~35 km (the talweg bathymetry shown in Figure 4 – inset a). Seventeen kilometers from its head, the canyon axis trend changes abruptly from N-S to NNE-SSW. The NNE-SSW trend of the canyon continues for 8 km and then changes to NNW-SSE (Figure 3a). The canyon's axial depth varies between 600 to 800 m, and its width from 3000 to 7000 meters (sections a-a', b-b', and c-c' in Figure 4). To the east of Canyon I, a narrow, steep-sided valley trending approximately N-S cuts into the margin for more than 9 km where it is transected and apparently offset, changing trend to NNW-SSE (white and black dotted line in Figure 3a). This valley joins Canyon I at 72°15'W (Figure 3a), reaching its maximum width of ~6 km at this point (section c-c' in Figure 4). These canyons no longer appear to be extensions of a present-day coastal river, as they have been disconnected by the offset of the SOFZ (Leroy et al., 2015).

Another channel runs approximately NW-SE along the northern shore of Tortue Island and intersects Canyons II and III (Figure 3a, Oliveira de Sà et al. 2025). Approximately 10 km from the canyons' heads toward the north, Canyons II and III are both deflected along the trend of this channel, by a fault (Figure 3a). Canyon II's trend is sinuous at the deflection but returns to its original NNE-SSW trend downslope. Canyon III's trend is only slightly deflected, continuing with a more NNW-SSE trend downslope (Figure 3a). All canyons present U-shaped profiles and similar geomorphological evolution (sections a-a' to f-f,' in Figure 4 – inset a).

Several N–S rectilinear channels incise the northern insular slope (Figure 3a). The head of these rectilinear channels coincides with the location of the NW-SE trending strike-slip fault that deflects the Canyons II and III (Figure 3a). The longitudinal profile of the inactive canyon (Figure 4) shows the reverse fault drawn in Figure 3.

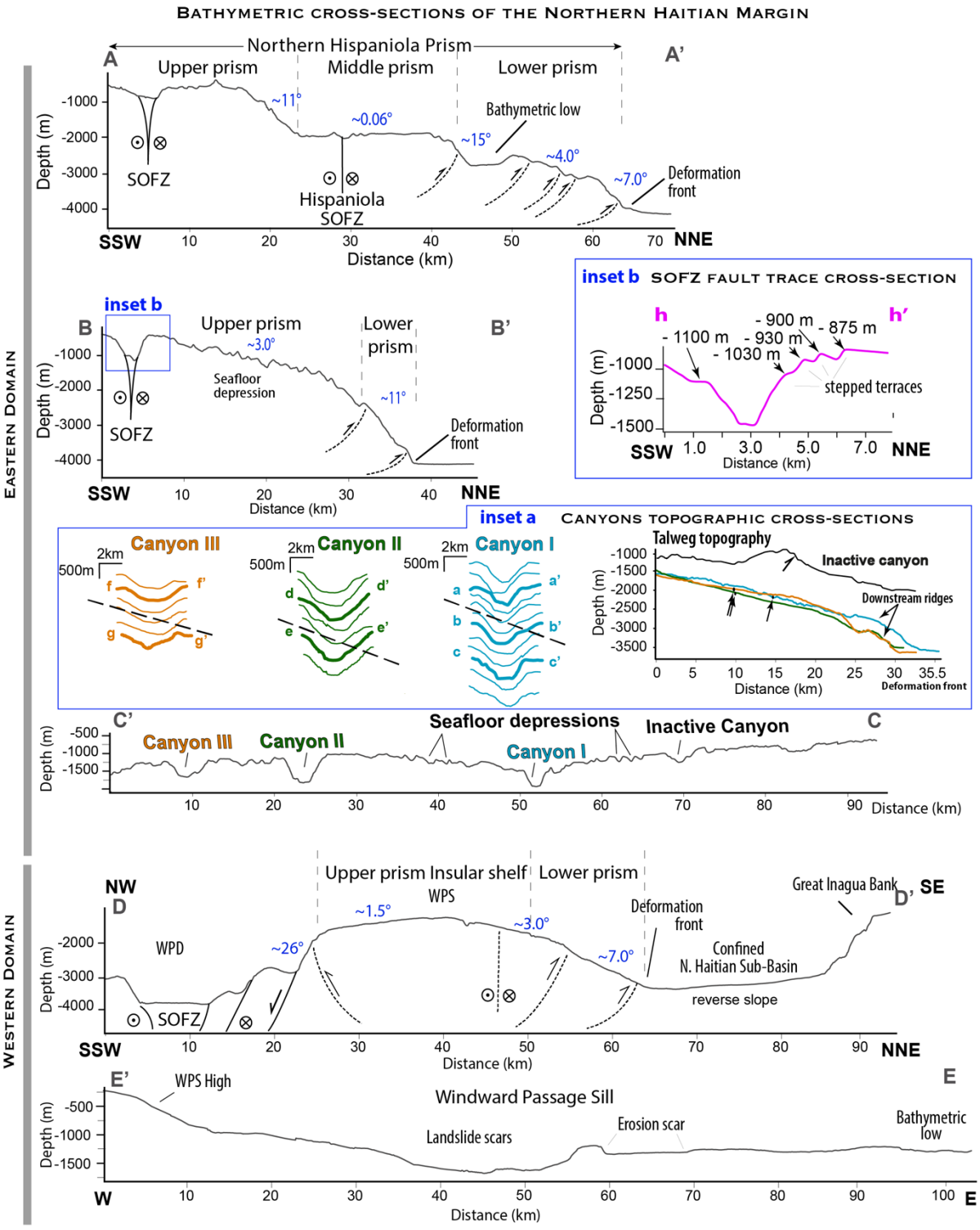

Figure 4: Bathymetric analysis of the eastern and Western domains of the Northern Haitian margin. Bathymetric cross-sections with morphological analysis of surface features (canyons, depressions, scars, terraces) and schematic positioning of structural features at depth (strike-slip, thrusts). See Figure 3 for profile locations. A-A'; B-B' and, D-D' cross-sections show the Northern Hispaniola Prism with its lower, middle, and upper prism parts. The offshore extension of the on-land Hispaniola SOFZ cuts the middle prism. The N. Haitian sub-basin exhibits a reverse slope, whereas the Caicos sub-basin is flat. Inset a: Bathymetric cross-sections across Canyons I, II, and III. See Figure 3a for location. Profiles a-a' to g-g' show the thalweg bathymetry along the three canyons. Dashed lines are the strike-slip faults location.

Blue is Canyon I; green is Canyon II, orange is Canyon III, solid line: the inactive canyon. Inset b: Cross-sections of the fault SOFZ (Septentrional-Oriente Fault Zone) showing the stepped terraces. WPS: Windward Passage Sill. WPD: Windward Passage Deep.

4.3 Seafloor Depressions

The seafloor of the Eastern domain is affected by a closely packed set of alternating raised ridges and depressions filled with ponded sediments (section C-C' in Figure 4). They are kilometer-scale features that appear in water depths ranging from 600 m to 2000 m (Figure 3a – inset). The narrow-raised ridges that define individual walls of these structures have a complex morphological pattern, which gives rise to shapes ranging from circular to irregular (Figure 3a – inset).

The Western domain has broad bathymetric lows and scars (Figures 3b and 4, section E-E'). There are no indications of seafloor depressions at the WPS (Figure 2b). The depressions are only located in the Eastern domain in the ~2224 km^2 area northeast of Tortue Island (Figure 3a).

4.4 Seismic stratigraphy

Seismic units are named and ordered from the acoustic basement to the most recent Unit 4, as proposed by Oliveira de Sá et al. (2021) in the Windward Passage region.

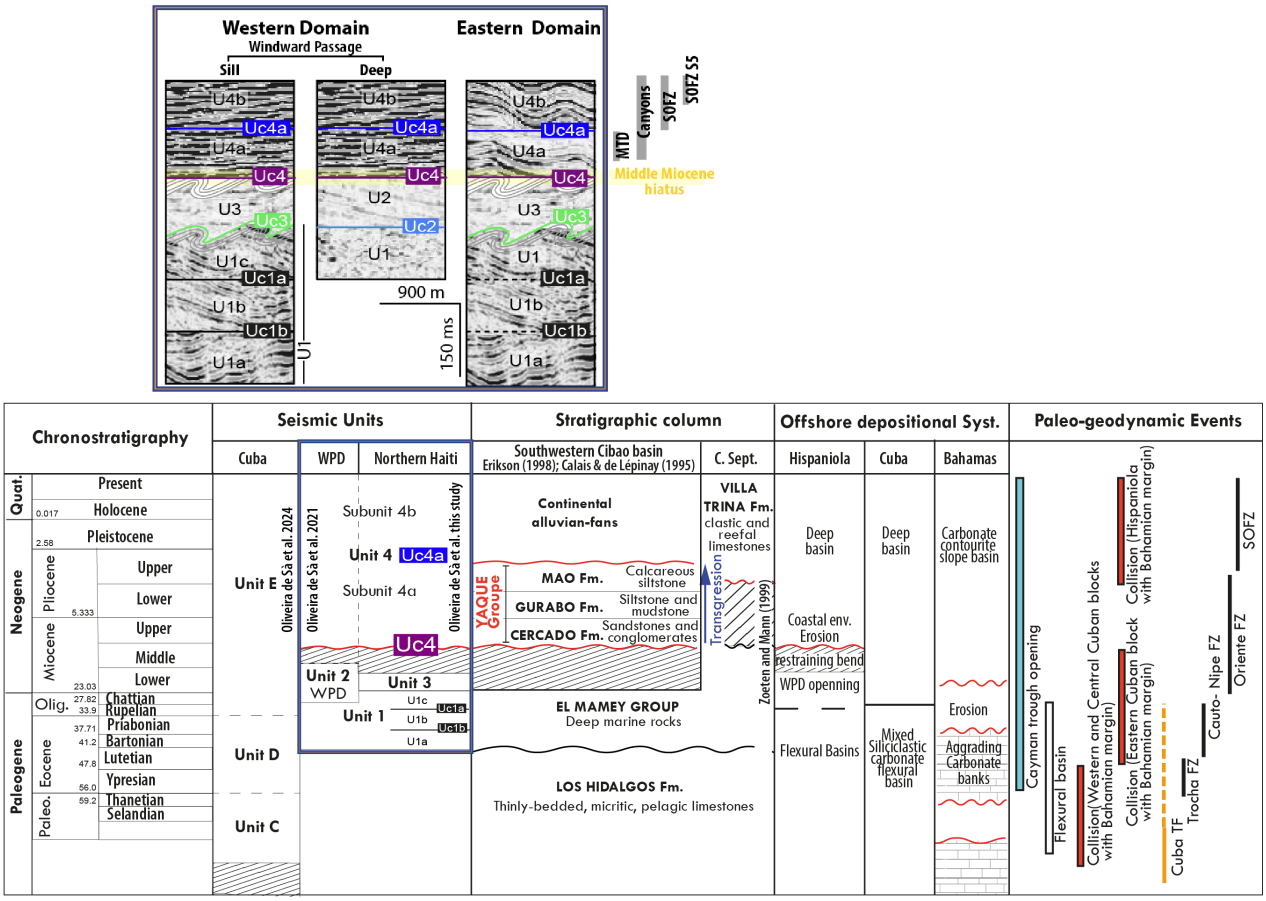

Figure 5: Diagrams illustrating a synthetic log of the seismic units and their seismic patterns (Upper panel). Age estimates of these units are provided, as well as the timing of the MTD emplacement, the initiation of the incising canyons, the establishment of the Septentrional-Oriente Fault Zone (SOFZ), and its most recent S5 segment. The lower panel displays the same seismic unit (framed in blue) as those identified in northern Cuba (Oliveira de Sà et al. 2024). We also present the stratigraphic column of the Southern Cibao basin and the Cordillera Septentrional, along with the offshore depositional systems and the paleo-geodynamic events of the area.

Interpretation of these units at the northern Haitian margin is based on throughgoing correlation and cross-referencing with profiles located in the Windward Passage area (Figure 5; Oliveira de Sá et al., 2021). The quality of the seismic signal is, for the most part, insufficient to accurately image the reflectors of Units 1 and 3 in the Eastern domain, revealing only the reflectors in the uppermost parts of these units.

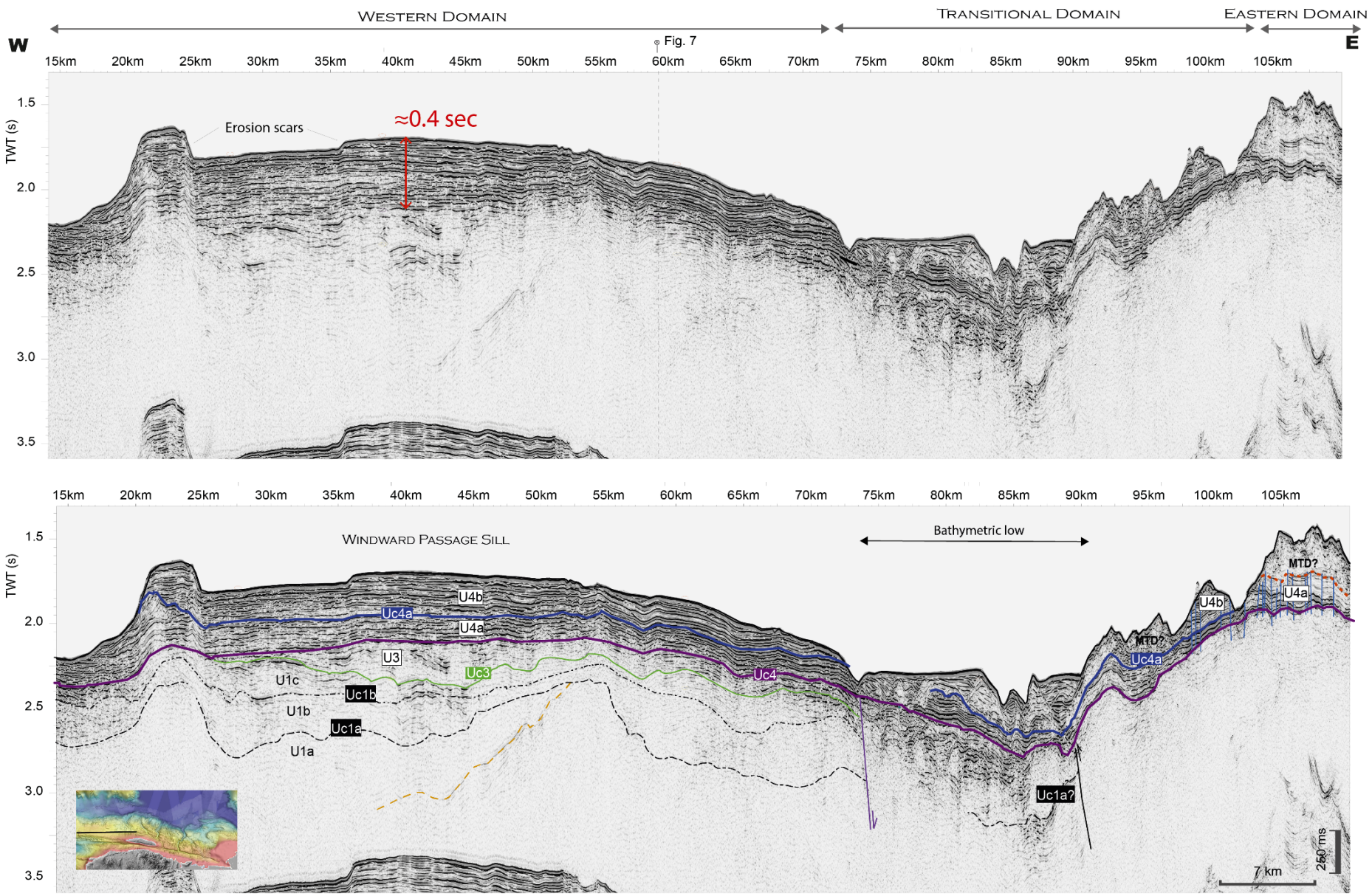
WESTERN DOMAIN
TRANSITIONAL DOMAIN
EASTERN DOMAIN
W
E
Fig. 7
15km 20km 25km 30km 35km 40km 45km 50km 55km 60km 65km 70km 75km 80km 85km 90km 95km 100km 105km
TWT (s)
1.5
2.0
2.5
3.0
3.5
Erosion scars
≈0.4 sec
WINDWARD PASSAGE SILL
Bathymetric low
U4b
Uc4a
U4a
U3
Uc3
Uc4
U1c
Uc1b
U1b
Uc1a
U1a
MTD?
Uc1a?
7 km
250 ms

Figure 6: Seismic line H12-122. At the top, the uninterpreted seismic line with a W-E orientation illustrates the Western and Eastern domains of the study region, as well as the transition zone between these two domains, which corresponds to the location of a bathymetric low. See location in Figure 2a.

In the Western domain, Unit 1 (U1) consists of a relatively thick series (0.4 - 0.8 s TWT) with two internal angular unconformities (Uc1a and Uc1b) that separate sub-units with distinct facies and geometries (U1a, U1b and U1c, Figure 5). The sub-units within U1 and their associated unconformities are discernible in Figures 6 and 7, km 23-35, and can be seen in the correlation plot of the seismic profiles extending towards the western region (e.g., Figure 7 of Oliveira de Sá et al., 2021). However, they remain faint on the seismic profiles due to the attenuation of the seismic signal.

Unit 2 (U2) is not identified in the study area. This unit was described by Oliveira de Sá et al. (2021) only in the WPD (Figure 2). This syn-tectonic unit is associated with the opening of the Windward Passage between Cuba and Hispaniola (Oliveira de Sá et al., 2021).

Unit 3 (U3) is characterized by tilted and folded reflectors, filling the syncline depressions formed by prior folding of U1 (Figures 6, 7, and 8b; Oliveira de Sá et al., 2021). U3 is delimited at its top by the Uc4 unconformity (purple).

Unit 4 (U4) shows well-stratified and high-amplitude reflections in the west of Tortue Island (Figures 6, 7, and 9). Towards the east, the horizontally layered, high-frequency reflectors of U4 become complex internal reflectors separating layers of greater thickness (Figure 3, depth to Uc4 map; Figure 9, km 80-140). Subparallel, wave-like seismic reflections in this area characterize U4. U4 is divided into two subunits: U4a, and U4b. U4a is bound by unconformities Uc4 (purple) and Uc4a (blue) (Figure 6). The strata thickness varies across the study area, thickening towards the east (≈0.4 sec westward, ≈0.75 sec eastward; Figures 6 and 9).

Within the Western domain, U4a is characterized by continuous and parallel high-amplitude reflections from Uc4 to Uc4a (Figure 9 km 0-30). Within the Eastern domain, the lower portion of U4a is marked by a layer showing continuous high-amplitude reflections (Figure 9). This high-amplitude layer exhibits a double-wedge shape, thickening as it approaches the central axis of Canyons II and III that incise U4 in the Eastern domain (Figure 9, km 80-110 and km 112-130). Except for the channel-fill, this layer is relatively thin and the signature at some locations is characterized by the two continuous high amplitude reflections from its top and base (Figure 9 between km 120-125). The internal seismic pattern of U4a from Uc4 to Uc4a, is characterized locally by relatively continuous, parallel, high to moderate amplitude reflections (Figures 9, km 135, Figure 10 km 3 to km 5, Figure 11 km 0 to km 1.5). Vertically and laterally, the facies change from well-bedded, visible reflections to more transparent ones. This particular unit is interpreted as an MTD. The lower limit of this MTD is marked by Horizon A (dotted orange line Figures 10, 11, and 12), and its upper limit by Horizon B (dotted green line Figures 10, 11, and 12).

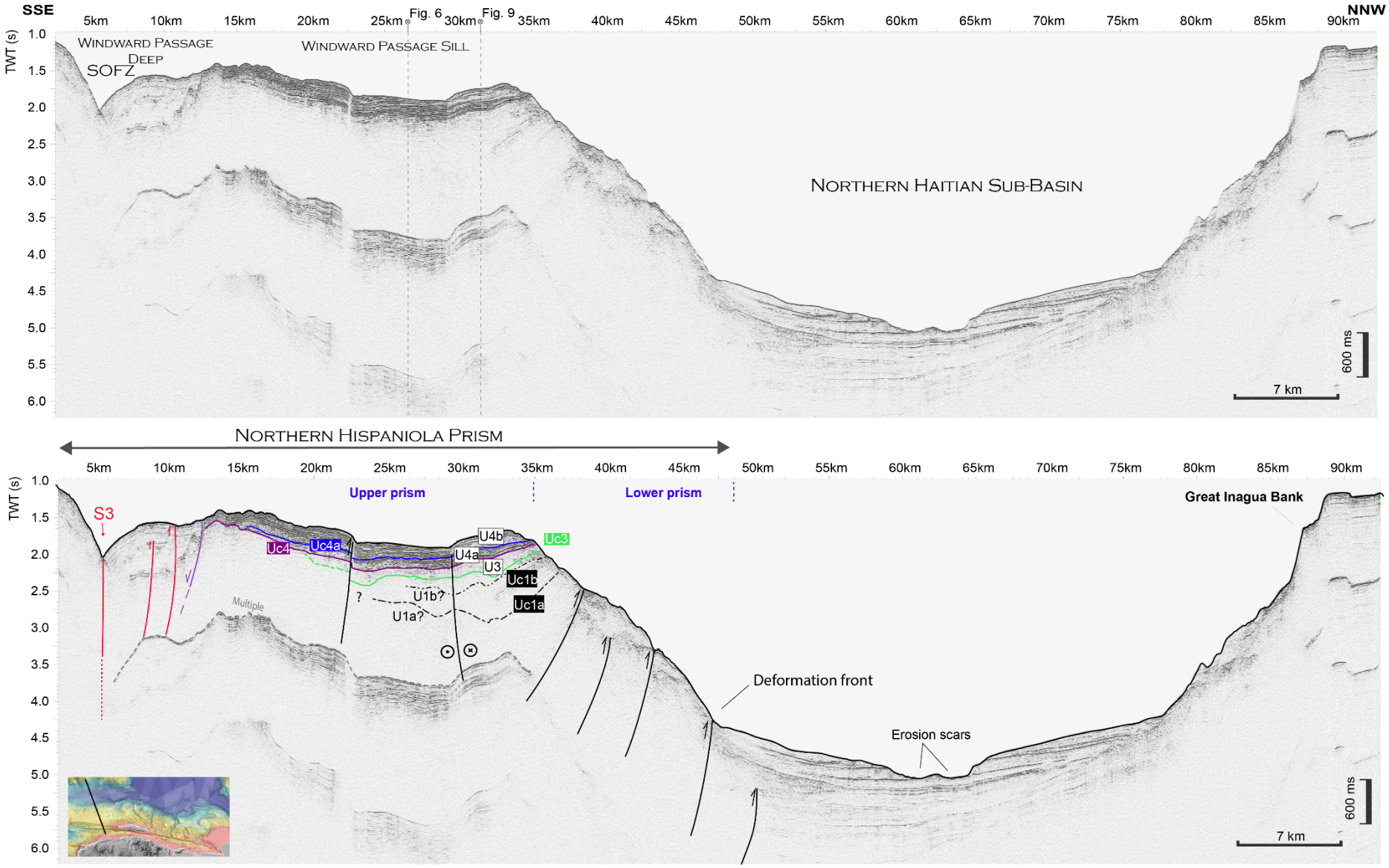
SSE
NNW
Fig. 6
Fig. 9
5km
10km
15km
20km
25km
30km
35km
40km
45km
50km
55km
60km
65km
70km
75km
80km
85km
90km
TWT (s)
1.0
1.5
2.0
2.5
3.0
3.5
4.0
4.5
5.0
5.5
6.0
Windward Passage
Deep
SOFZ
Windward Passage Sill
Northern Haitian Sub-Basin
600 ms
7 km
Northern Hispaniola Prism
Upper prism
Lower prism
Great Inagua Bank
S3
Uc4
Uc4a
U4b
U4a
Uc3
U3
Uc1b
Uc1a
U1b?
U1a?
?
Multiple
Deformation front
Erosion scars

Figure 7. Seismic line H12-146. At the top, the uninterpreted seismic line crossing the Western domain of the study region displays the WPS and the Haiti sub-basin. Dashed lines correspond to intersections with the other seismic profiles. At the bottom, the interpreted seismic line shows the reverse faults on the lower prism, as well as the westward continuation of the strike-slip fault that offsets the path of the canyons from the Eastern domain, and reverse faults (km 20.5) affecting the most recent sedimentary cover. See location in Figure 2a. The vertical dashed lines correspond to the crossing line, and the solid vertical line to the crossing seismic line is shown in Figure 9.

In the Eastern domain, the MTD truncates the top of U4a (Figures 10, 11, and 12). It is characterized by internal transparent to chaotic seismic facies, although some continuous reflections can be seen within this deposit (Figures 10, 11, and 12). The MTD truncates the U4a across almost the entire extent of the Eastern domain.

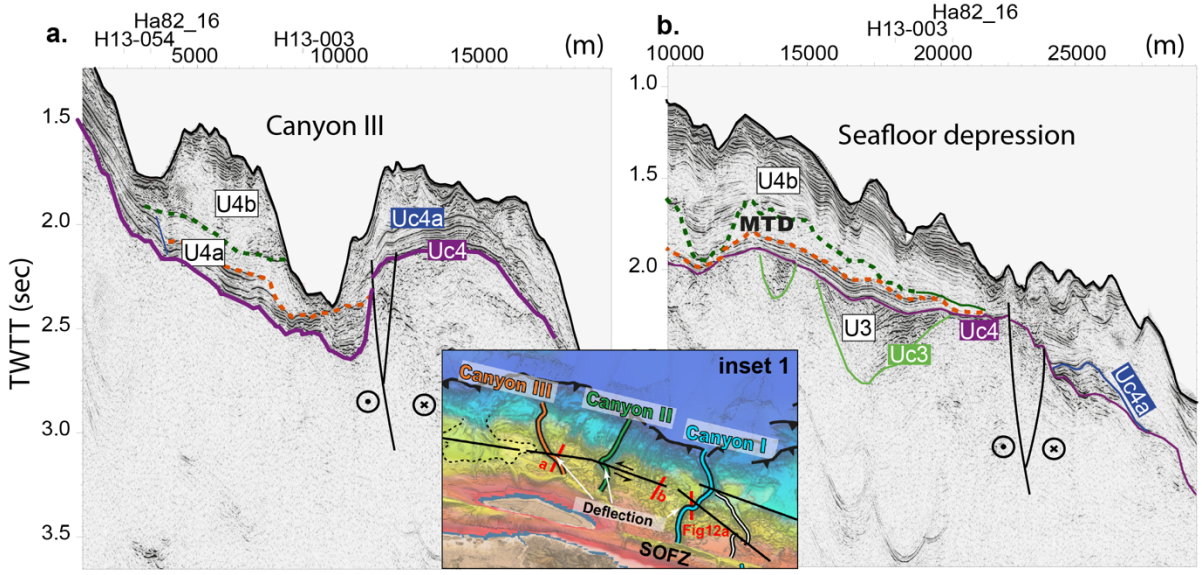

Figure 8. a) Seismic line H12-149, and b) Seismic line H12-124. The figure shows segments of these seismic lines showing the presence of deep strike-slip fault system that seem to be related to the deflection and offset of canyon paths visible on bathymetric maps. As can be seen in Inset 1, the canyon deflections and offsets correspond to the position of this strike-slip fault system.

Some amplitude anomalies are found above U4a, such as the V-shaped anomaly consists of two bedding-concordant limbs dipping towards a shared basal apex (Figures 9 "wing" km 120 and 12b – inset 1). The limbs of these "wing-like" reflections are discordant to the surrounding stratal reflections (Figure 12b – inset 1).

U4b constitutes the uppermost stratum of the sedimentary fill in the Northern Haitian margin (Figure 9). In the Western domain, U4b is bound by the basal unconformity Uc4a (blue) (Figures 5 and 9). Here U4b displays well-stratified high-amplitude reflections (Figures 7, 8, and 9). The thickness of U4b varies throughout the study area. In the Eastern domain, the U4b is thicker and bound at its base by Uc4a or Horizon B at the top of the MTD when present. Thus, Horizon B, where present, represents the base of U4b and the top of the MTD (Figures 9 and 10). In the Eastern domain, the upper part of the U4b is cut by numerous seafloor depressions, present throughout this domain (Figures 3 – inset, 9, 10, 11, 12, and 13). The reflectors have a complex, wave-like geometry (Figure 9 – inset). The amplitude of the reflectors is higher at the top of the unit, transitioning to lower amplitude reflectors at greater depths (Figures 9 and 10). Horizon B onlaps the basal reflectors of the subunit U4b, forming a highly undulated contact (Figure 10 – inset 3).

4.5 Deformation Front

The sediments of the Northern Hispaniola Prism have been progressively deformed by imbricate thrust faults, forming narrow and smooth E-W trending anticline ridges on the seafloor that suggest active deformation in this area (Figure 2b). These thrust faults imbricate the thicker Caicos sub-basin infill (Figures 10 and 13). The prism can be followed toward the east along the northern Dominican Republic, where it has been referred to as the Northern Hispaniola Deformation Belt (Rodriguez-Zurrunero et al., 2020), and to the west into the Old Bahamas Channel that runs along the northern Cuban coast (Figure 1; Oliveira de Sá et al., 2024). However, the geometry of the deformation front and the extent of the prism varies from Eastern to Western domains.

The deformation front shows two pronounced undulations between 73°W and 71°30'W (Figure 2b). Offshore of the Dominican Republic (71°40' to 72°20'W) in the Eastern domain, the margin stretches out for almost 70 km. The seafloor here displays an irregular pattern of prominent ridges and intervening lows (section A-A' Figures 3a and 4). In this area, the prism is characterized by three distinct tiers (upper, middle, and lower) (section A-A' Figure 4). The upper prism corresponds to the insular shelf, the middle prism corresponds to a plateau midway down the insular slope, and the lower prism extends to the deformation front (Figures 1, 4, and 13). In contrast to the lower prism, the middle prism appears to be slightly deformed with no significant thrust faults. The upper prism is crossed by the SOFZ (Figure 4). North of the Tortue Island, the Northern Haitian margin narrows to ~30 km, with only the lower and upper prisms present (section B-B', in Figures 4 and 10). The vergence of the imbricate thrust faults is slightly northeast (Figures 4 and 13). Further north, far from the ridges, the deep Caicos sub-basin floor is smooth and flat.

In the western region (from 73°W westward) encompassing the WPS, the deformation front exhibits a more linear east-west orientation (Figure 2b). It is characterized in seismic profile by tightly folded thrust sheets interpreted as belonging to the lower prism domain (Figure 7). Some of these thrusts are overlaid by sediments from the slope, concealing this not very active north-trending imbricate system (Figure 7). The WPS corresponds to the upper prism in the continuity of the insular shelf.

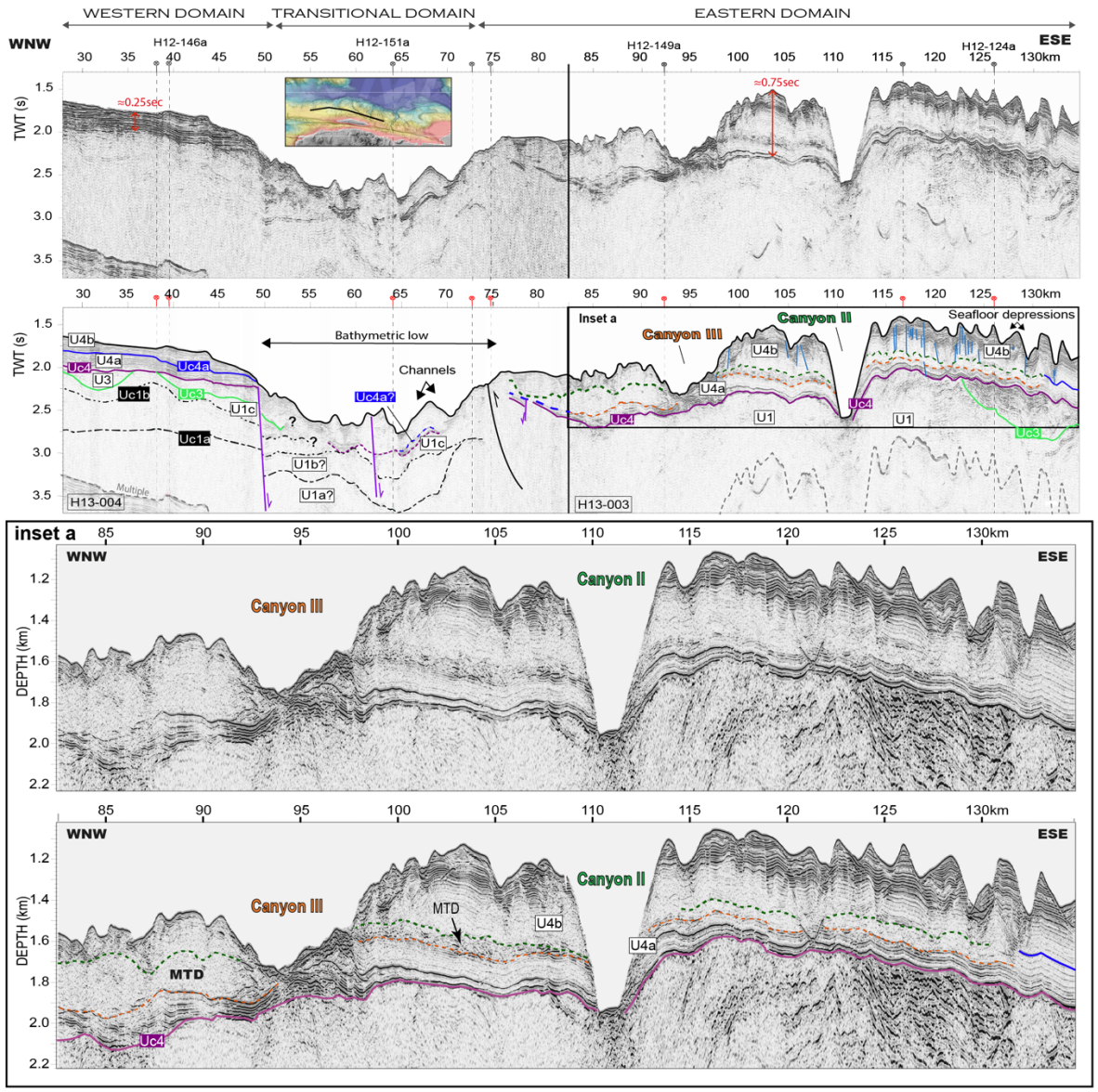

Figure 9: Combined seismic line from seismic profiles H13-003 and H13-004. W-E trending seismic profile of the northern Haitian margin. See location in Figure 2a. Dashed line and red dots show the intersections with other seismic profiles. Inset a: detailed of U4 showing the fault network and the attenuation of the amplitude of U4 reflections with depth. Inset a: the seismic profile has been converted to depth using the following velocity law. From 1500 to 2000m/s at the Uc4 unconformity and from 2500 to 4000m/s at the base of the selected profile.

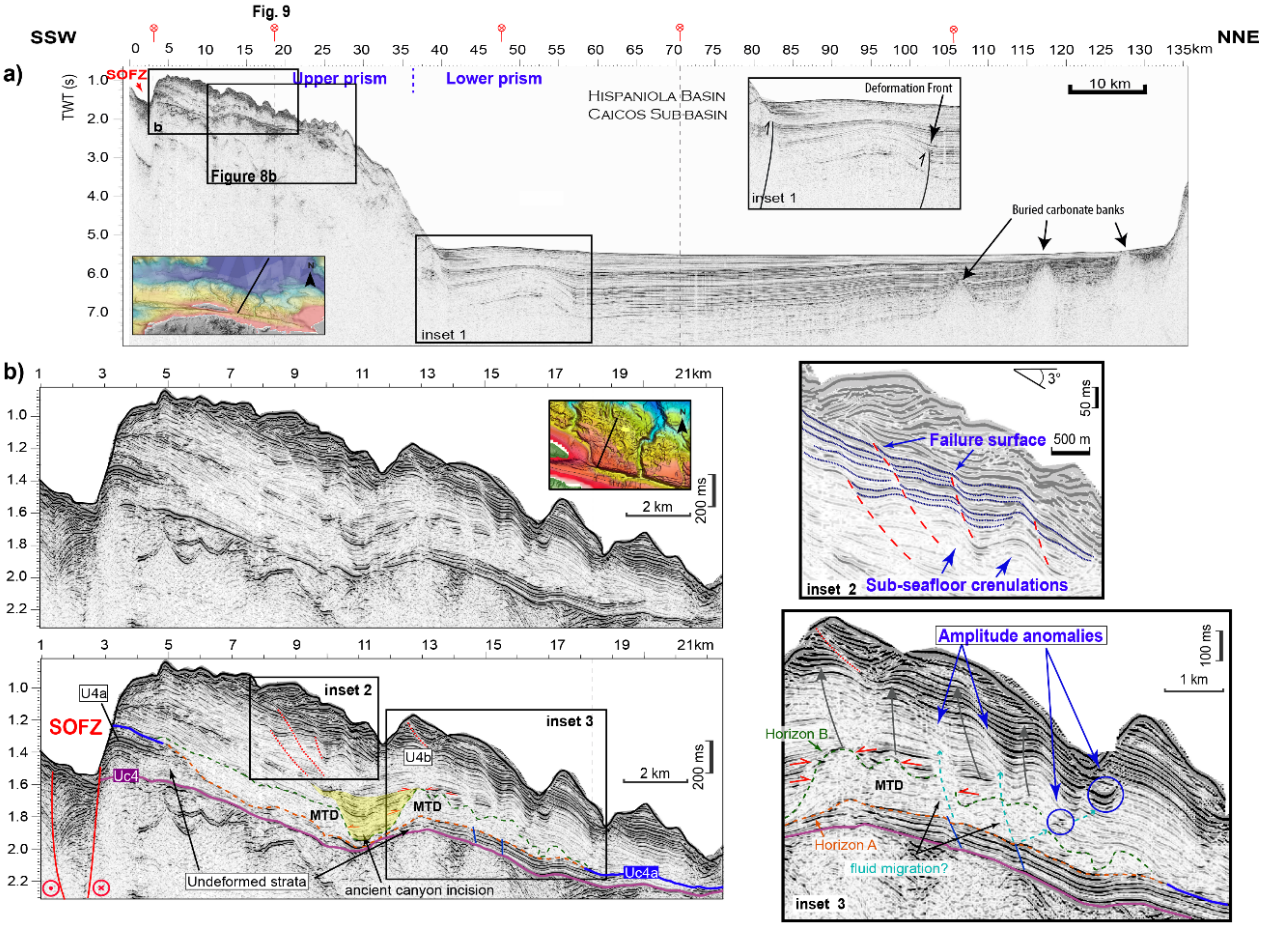

Figure 10. Seismic line H12-124. a) Uninterpreted seismic profile showcasing the northern prism of Hispaniola and the Caïcos sub-basin. Buried carbonate mounts are indicated at the northern tip of this basin. See location in Figure 2a. b) Close-up of the recent sedimentary cover of the upper prism. The MTD deposit is highlighted, along with the valley shaped by the trace of the SOFZ. Inset 1: Close-up on the frontal fault (deformation front) showing that this fault does not propagate into the most recent deposits of the Caïcos sub-basin. Inset 2: Displays condensed zones within the sediment waves affecting the reflectors of the U4b subunit, creating subsurface crenulations. Inset 3: Close-up on the distal part of the MTD, which appears more chaotic. The reflectors of the U4b unit onlap the MTD and seem to be "whitened" by potential fluids migrating upwards from the MTD. These fluid exits are inferred by the local amplitude loss of the U4b unit reflectors in contact with this MTD. Grey-coloured arrows indicate that the reflectors of unit U4b mimic the reliefs of Horizon B.

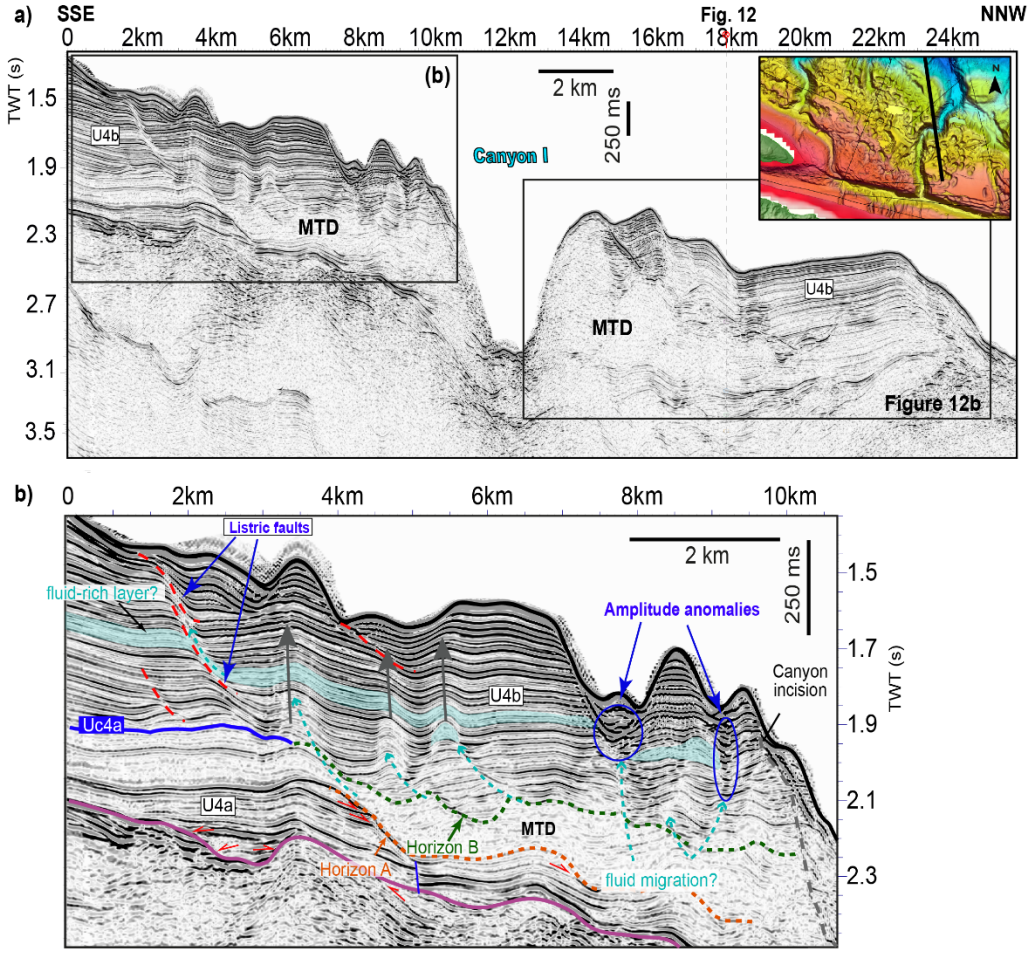

Figure 11. Seismic line H12-128. a) Uninterpreted seismic line displaying Unit 4 impacted by depressions on the seafloor of the eastern domain of the study region. See location in Figure 2a. b) Close-up on Unit U4 showing the MTD continuous with sub-unit U4a. Amplitude anomalies are visible at the top of the MTD, from which fluids appear to be migrating upwards. Grey-coloured arrows indicate that the reflectors of unit U4b mimic the reliefs of Horizon B.

5. Discussion

Summary of Results

The northern Haitian margin presents two distinct domains: the Eastern domain extending from Christi Islands to Tortue Island and the Western domain south of the Great Inagua Bank, including the area west of Tortue Island and Punta Maisi in Cuba. Seafloor morphology varies significantly between the two domains, with the Eastern domain featuring deeply incised canyons notably associated with the SOFZ, seafloor depressions, terraces, and anticlinal ridges. In contrast, the Western domain displays broader bathymetric lows and erosion scars. Seismic stratigraphy reveals four units, with U4, subdivided into subunits U4a and U4b, displaying complex internal reflectors. Additionally, a buried MTD is identified within U4a in the Eastern domain, truncating the stratigraphy and exhibiting complex internal seismic facies. The deformation front in the Northern Haitian Prism exhibits imbricate thrust faults, forming anticline ridges indicative of active deformation, with variations observed between the Eastern and Western domains. Moreover, the morphology of the broad, flat Caicos sub-basin is distinctly different to the narrow, southward-sloping Northern Haitian Basin, which is confined between the Windward Passage Sill and the Great Inagua Bank.

5.1 Stratigraphic record and seafloor morphology variability

In both Eastern and Western domains, the seismic units underlying Uc4 show comparable architecture indicating similar deposition and deformational histories from the late Oligocene until the middle Miocene (Calais and de Lépinay, 1992; Oliveira de Sà et al 2021). However, the thickness and internal architecture of U4 in the Western domain varies significantly from that in the Eastern domain, indicating distinct deposition histories and evolutions from the middle Miocene to the Present.

The high-amplitude and well-stratified reflection pattern within U4 in the Western domain (0.4 s TWT thick, Fig. 6) presents a marked contrast with the complex wave-like pattern of seismic reflectors within the thicker U4 in the Eastern domain (0.75 s TWT thick, Figure 9). In particular, the occurrence of a high-amplitude layer at the base of U4a and the MTD at the base of U4b, is documented exclusively within the Eastern domain. Moreover, U4b exhibits wave-like internal reflections and a greater thickness in the Eastern domain than in the Western domain (Figures 10, 11, and 12).

The distinct post-middle Miocene stratigraphy of the Eastern and Western domains points to significantly different tectonic settings and lead to different sedimentary deposits. The middle-Miocene collision of the Western domain with the Bahamas Carbonate Province (Rojas-Agramonte et al, 2005) accompanied by the opening of the Windward Passage and motion on the OFZ shifted the depositional environment from deep-water accretionary prism, still present in the Eastern domain, to a collisional regime.

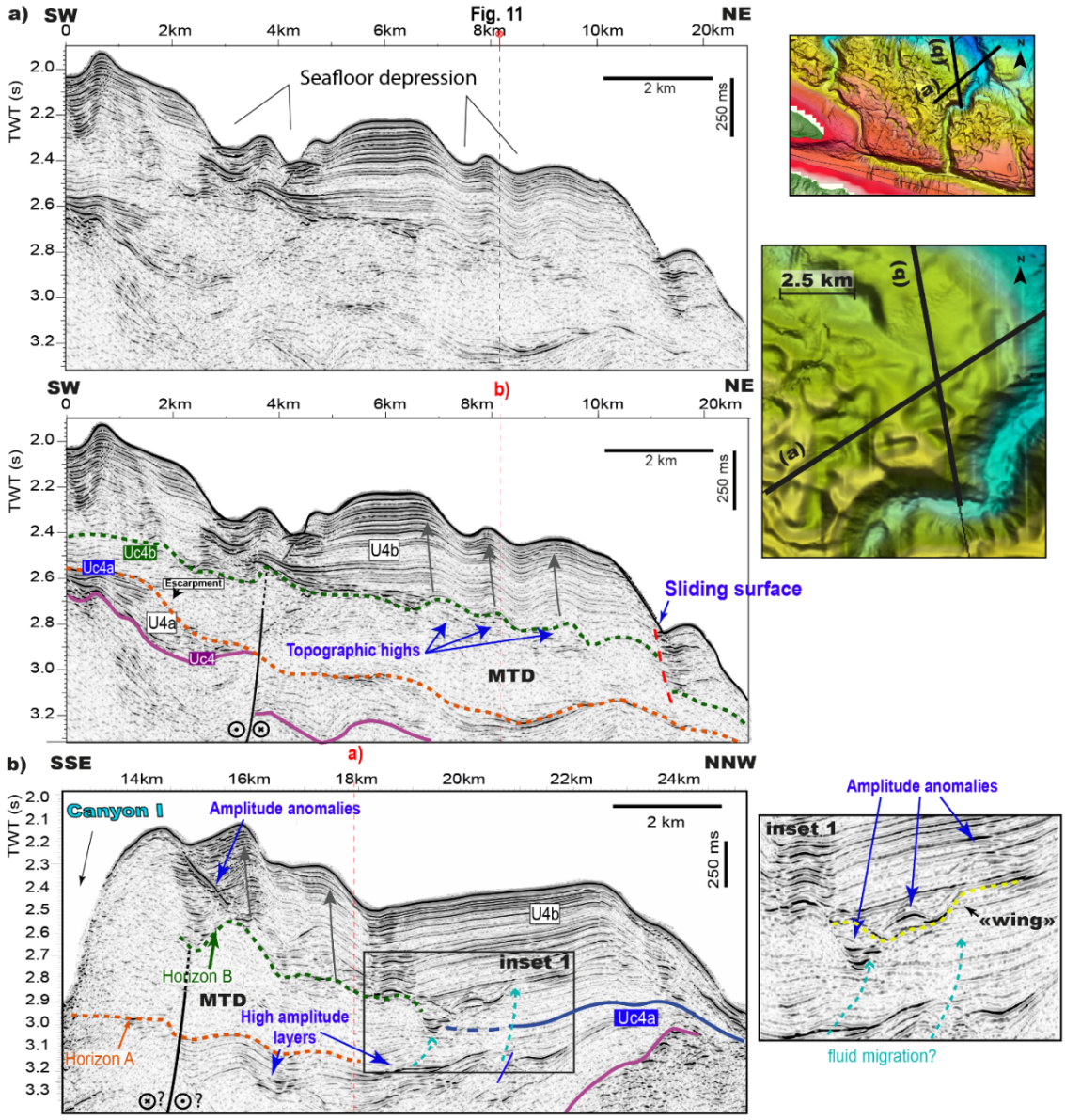

Figure 12: a) Seismic line H13-002. At the top, an uninterpreted seismic line shows U4 impacted by depressions on the seafloor of the Eastern domain of the study region. See location in Figure 2a. At the bottom, the interpreted seismic line displays the wavy geometry of Horizon B, which defines the top of the MTD. b) Profile shown on a larger scale in Figure 11a. Inset 1 displays amplitude anomalies typical of sandy intrusions, known as "wings". Grey arrows indicate where the reflectors of U4b mimic the reliefs of Horizon B

5.1.1. Evidence of post-depositional remobilization within Unit 4

The high amplitude reflectors identified at the base of U4a could indicate the early deposition of sand-rich strata (Ma et al., 2020). The presence of significant sandstone-bearing units in the study area cannot be confirmed as no sediment cores long enough have been logged. However, Middle/Late Miocene up to middle Pliocene deposits in the Cibao Basin (Figure 1b – step c, Yaque Group, e.g., Erikson, 1998; Escuder-Virruete et al 2.020) show successions of thick intervals of sandstone and conglomerate deposits (middle neritic to upper bathyal) (Erikson, 1998). The Cibao Basin can be considered, in a paleogeographic reconstruction, as the proximal part of the study area during the Pliocene (Figure 1b). These deposits are likely associated with a large channel-levee system that transported sand and other sediments derived

from the Central Cordillera and the uplifting and eroding Septentrional Cordillera (Figure 1b and c). Analogous sand-rich deposits are also found on the adjacent coast of Tortue Island, where sand-rich deposits prevail (Figure 1a) (Cotilla-Rodríguez, 2021). Furthermore, the double-wedge shape thinning away from the channel fill in Figure 9 can be interpreted as external channel levee deposits, which develop adjacent to channel belts (Kane and Hodgson, 2011; Saller and Dharmasamadhi, 2012; Shepard, 1965). As described by Calais et al. (2016); Escuder-Viruete & Pérez (2020), a collisional episode of Hispaniola with the Bahamas Carbonate Province beginning in the late Pliocene resulted in folding, faulting and uplift of the Septentrional Cordillera. We suggest that the U4a sand-rich deposits, formed during the Middle/Late Miocene up to the Middle Pliocene when the study region would have been characterized as a deep depositional environment, acted as a source of fluids (Figure 1b) (Erikson et al., 1998). Excess pore fluid pressure within buried sand strata can arise from differential compaction, fluid buoyancy, lateral pressure transmission, and silica diagenesis (Davies et al., 2006; Huuse et al., 2007; Osborne and Swarbrick, 1998). This renders these formations vulnerable to displacement and injection in case of seal layer failure (Gay et al., 2004; Hurst et al., 2003; Monnier et al., 2014). A common characteristic of remobilized and injected sands is the presence of wing-like sandstone intrusions (e.g. East Greenland, Surlyk et al., 2007; Northern England, Kane, 2010; Barents Sea, Safronova et al., 2012). These features can assume diverse configurations, ranging from dike-like structures to dikes culminating in sills (Monnier et al., 2014). These sandy injections propagate outward from their origin through conduits and occasionally traverse the sedimentary layers, intersecting different stratification planes within the rock (Jackson, 2007; Kane, 2010; Lonergan et al., 2013). "Wings" are observed in seismic data as prominent high-amplitude reflections originating from sandy bodies. The observation of wing-like anomalies atop the high amplitude basal layers of U4a, coupled with the existence of minor faults that subtly disrupt the reflectors within U4, likely attributed to the effects of differential compaction, strengthens the proposition of an excess of fluid pressure in a sandstone lower level (Figures 10, 11 and 12).

5.1.2 Significance of the MTD in the Eastern Domain

The position of the MTD above Uc4 and in lateral continuity with the undeformed strata of U4a suggests that the MTD deposit affects U4a only (Figures 11b and 12b). This is supported by the MTD being the same thickness as the laterally adjacent, undeformed interval of U4a. The presence of discernible reflectors inside the MTD (Figure 11b) supports the interpretation that the displacement was limited and that strata experienced minimal deformation near the leading edge. However, chaotic reflectors in the downslope direction show that it has undergone more significant deformation towards the north (Figure 10 – Inset 3). We interpret this as indicating that the MTD deposit was translated northwards down the slope (Figures 10, 11, and 12). Because of the presence of the sand injections, we hypothesize that U4a was subjected to pore fluid overpressure, a process known to have a negative effect on the stability of marine slope sediments (Locat and Lee, 2002).

The absence of the MTD in the Western domain might be considered by two processes. The first is primarily tectonic, regarding the vertical movements and associated instabilities linked to the collision with the Bahamas Carbonate province. Then, the absence of the MTD in the Western domain might be due to its more remote position from the northern coast of the Dominican Republic, which collided with the Bahamas Carbonate Province during the Late Pliocene (Escuder-Viruete & Pérez, 2020). If this is the case, the Western domain was less tectonically active than the Eastern domain during this period. The Eastern domain corresponds to the offshore extension of the Septentrional Cordillera (Figure 1) and was subjected to intense tectonic activity. The other explanation for the absence of MTD in the Western domain may

also be attributed to a smaller sedimentary flux, which is a more likely interpretation as the sediment sources are further away (Figures 3 and 14, green arrows, Cuba, Haiti, Tortue Island). Indeed, the greater thickness of U4b in the Eastern domain would further corroborate higher sedimentation rates, which could have been responsible for larger sediment loads that would have exceeded sediment resistance. Based on the location of the MTD between U4a and U4b, a Late Pliocene age can be proposed. Considering that the collision between Hispaniola and the Bahamas (e.g., Calais et al., 2016) started in the Late Pliocene, it seems reasonable to link the MTD triggering to the combination of tectonics, earthquakes and subsequent liquefaction and post-depositional remobilization of U4 at that time.

5.1.3 Wave-like pattern of Subunit U4b

The bathymetric lows of the rugged Horizon B at the top of the MTD are filled with relatively homogenous sediment of U4b, which displays lower amplitude reflectors at its base and higher amplitude at its top (Figures 11 and 12). U4b entirely covers MTD and its seismic reflection pattern mirrors the rugosity of Horizon B (Figures 10, 11, and 12). A variety of mechanisms could have produced this wavy architecture including differential compaction, sliding or creep, or deposition of sediment waves by bottom currents.

Differential compaction during early burial tends to occur in association with variations in lithology, which impose unequal rates of mechanical compaction in strata (Davies, 2005; Herbert, 1993). Differential compaction seems to have occurred over the more disaggregated (chaotic reflectors) parts of the MTD. The less cohesive and loosely packed layers experience more pronounced compaction than the relatively solid blocks of less disaggregated layers. This process could lead to forced folding of the draping reflectors of U4b (Figures 8 to 12).

The areas where MTD exhibits chaotic reflectors also appear to be fluid-saturated with various amplitude anomalies in these locations (Figures 10 - inset 3, 11b, and 12 - inset 1). U4b may act as a seal, preventing fluids from migrating upwards from the MTD. On the other hand, the added weight of the overlying U4b may have increased fluid pressure within the MTD while the draping seal layers prevented fluids from migrating upwards, resulting in differential compaction within the MTD (Figure 11b). In spite of this, some fluids have escaped and evidence of their ascent appears as exaggerated folding of U4b reflectors (Figure 11b).

The draping reflectors of U4b are continuous and have a constant thickness over the top of the MTD (Horizon B in Figures 10, 11, and 12). Local depocenters and highs formed on the rough surface of Horizon B (Figures 10 – inset 3, and 12a). The depocenters are filled with the sub-horizontal reflectors of U4b, which onlap their inside walls (Figures 10 – inset 3 and 11b). Onlapping of concordant reflectors of U4b above Horizon B further suggests that it “folded” following deposition (Figure 10 – inset 3).

The bathymetric expression of these folds is maintained in the draped reflectors within almost the entire thickness of U4b, sometimes attenuating towards the upper part of the subunit. Occasionally, the crests and depocenters coincide with the folds on the flanks of the depressions. However, the presence of continuous layers identified on either side of the depressions indicates that they were formed by predominantly erosion processes (Figure 9 – inset, between km 112 and 125).

In the seismic profiles in which the MTD is not present (Figure 13) or where its top (Horizon B) is flatter (Figure 10, km 5-11), the folding of the reflectors in U4b is interpreted as associated with creep down the slope. Creep is a gravity-driven process, with the updip margins defined by retrogressively formed faults and folds (Lee and Chough, 2001; Li et al., 2016). Subaqueous creep has been observed on slopes steeper 3° (e.g., Shillington et al., 2012). Sliding surfaces associated with sub-seafloor crenulations within U4b (Figure 10 – inset 2) occur where the slope exceeds 3° (sections A-A', Figure 4). These surfaces could be related to growth folds, suggesting that the U4b is affected by creep and that the process can overwhelm the effects of

differential compaction of the MTD. These sliding surfaces do not appear to be linked to the differential compaction of the MTD since these features are observed even in areas where the MTD is not present (as in Figures 11 - km 0-2, and 13 – inset 1). Where these sliding surfaces are present above the MTD, the top of the MTD (Horizon B) is smooth (Figure 10).

On a large scale, the Eastern domain is characterized by a significant U4 sediment thickness (0.75 sec TWTT). U4 of the flat seafloor in the open Caicos sub-basin in the Eastern domain presents a contrast to that of the reverse slope of the North Haitian sub-basin in the Western domain (Figure 4 profiles A, B, D). In the Eastern domain, the base of U4 may act as a décollement surface. The undulating sedimentary features may result from hyperpycnal flows, which are commonly observed in nearshore bathymetric data (Lee et al., 2002; Mosher and Thomson, 2002; Urgeles et al., 2007; amongst others). In deep water, undulations can be produced by either deep-water turbiditic systems or by bottom currents (Lee et al., 2002; Rebesco, 2005). However, when significant discontinuity between seismic reflectors is associated with growth faults, these undulations are interpreted as having been formed by creep.

Each of these hypotheses, creep verses bottom currents, have supporting arguments: (a) most of the seismic reflections illustrate individual reflectors as quite continuous and no diffractions are visible on the synform part of the folds, which could indicate a rupture of the reflectors; (b) according to Urgeles et al. (2007) the regularity of the dipping of strata is better explained by sediment waves formed by bottom currents than creep. While we do not rule out the possibility that the wavy architecture results from the interaction between bottom current processes that form sediment waves locally disturbed by creep and differential compaction processes that could have affected post-MTD units. The resulting architecture of the MTD strata, which probably dates back to the Late Pliocene, continues to govern part of the contemporary seafloor morphology.

5.2. Tectonic Influences on the Submarine Canyons of the Eastern Domain

5.2.1. Influence of Deep Faults on Canyon Paths

In the Eastern domain, a network of submarine canyons stands out as a striking feature, while the Western domain is devoid of canyon incisions (Figure 3). The Eastern domain canyon system probably developed due to its immediate proximity to the northern coast of Hispaniola (Figures 2 and 3). The submarine canyons exhibit geomorphological attributes indicating that their morphology has been controlled by active tectonics. The canyons have been severed from the continental drainage system along the Haitian coast by the SOFZ (Leroy et al., 2015) and are no longer transporting sediments. However, deviations in the paths of the canyons suggest that their formations and evolution were probably structurally influenced while they were active (Figure 3a), as their paths seem to follow the left-lateral movement. Furthermore, no geomorphological elements (e.g., local bathymetric elevations caused by carbonate banks or seamounts) seem responsible for the deflection of the canyons. Instead, these bends appear to be related to the presence of faults at depth (Figures 8 and 12b). The lateral displacement of the canyons' paths may be due to strike-slip motion on a fault system within a transpressive tectonic setting. The effect of these faults on the bathymetry can be seen in the offset of the canyons. The now inactive canyon while it was being (white dots in Figure 3a) may predate the others and is probably used to connect the Hispaniola coast to the Caicos sub-basin. It has been inactive for some time, no longer carrying the sediment load that incised the margin. Unlike Canyons I, II, and III that continued to incise while being deflected, this inactive canyon was likely cut by a thrust fault that partially buried it (Figure 3a; Figure 4 inset, see longitudinal profile). The offset could envision the existence of the dextral strike-slip but is not truly compatible with the regional deformation style unless an NE-SW trending antithetic fault is present, as Escuder Viruete et al. (2020) proposed. However, this NE-SW trending fault does not appear in our data.

A more likely explanation could be that the thrust deforms the canyon path, thereby modifying its path (Figure 4; inset).

At ~20°0'N, the eastward deflection of Canyons II and III aligns with a left-lateral strike-slip fault as do the heads of the smaller rectilinear slope canyons (Figure 3a). It is interesting to note that the rectilinear slope canyon heads stop where they meet the fault (Figure 3a). The rectilinear morphology of these slope canyons is probably due to retrogressive headward erosion from the lower to the upper part of the slope (Figure 2) (Etienne et al., 2021). The fault may act as a barrier to their further progression upslope.

These faults are probably inactive or much less active than before; they do not have a clear imprint along the seafloor. However, their traces are inferred in the seismic reflection data (Figure 8), and from the deflection or offset of canyons by the ancient strike-slip motion parallel to the margin (Figures 3a and 8).

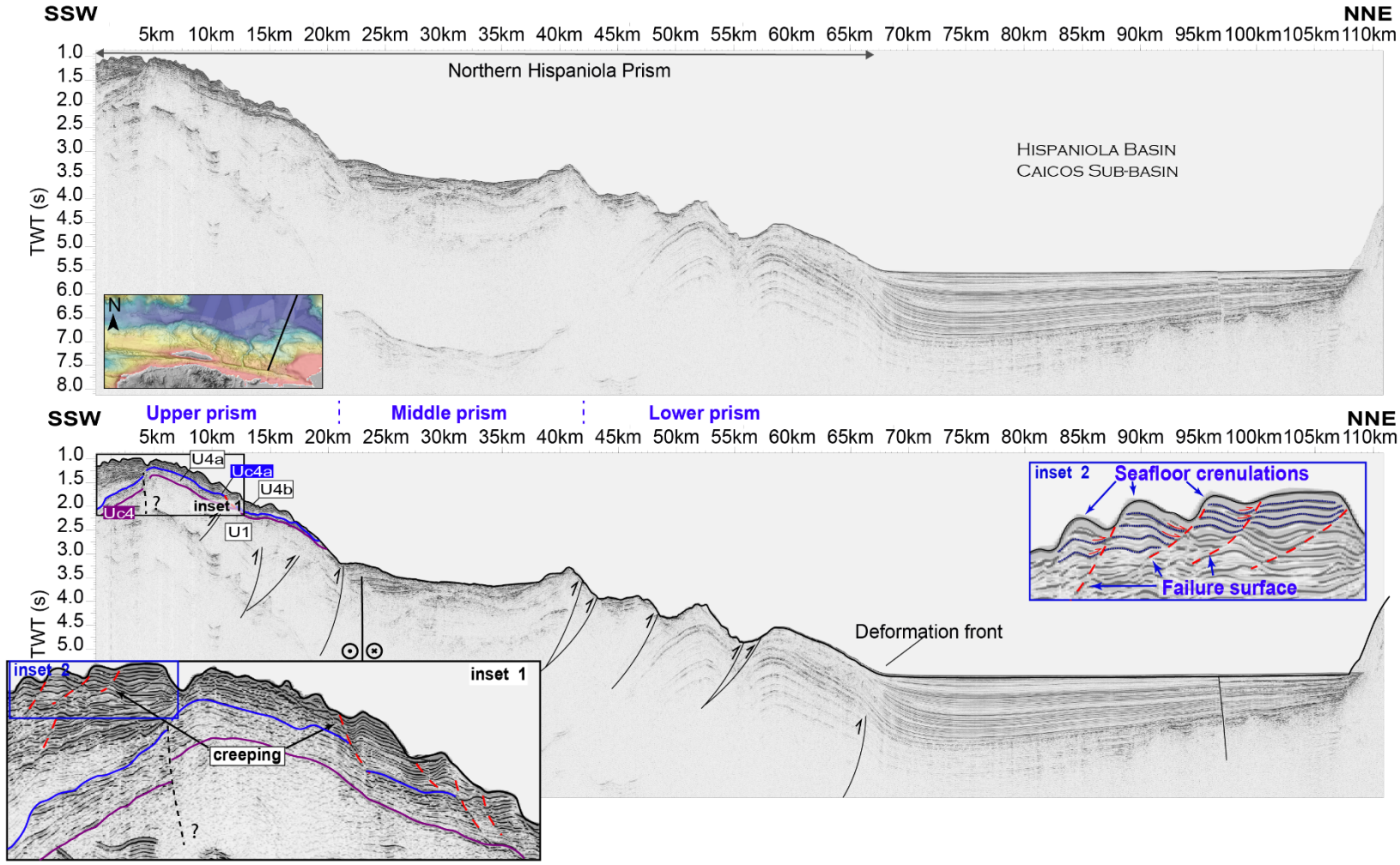

Figure 13: Seismic line H12-122a. At the top, uninterpreted seismic line through the Eastern domain showing the offshore North Hispaniola deformed belt. See location in Figure 2a. At the bottom, the interpreted seismic line and insets showing a close-up of the easternmost sedimentary cover of the upper prism. Here, the MTD deposit is absent, but sliding surfaces affect U4, creating crenulations within this unit and resulting in a very rough seafloor.

5.2.2 Influence of the deformation front on canyon morphology

The submarine canyons identified within the Eastern domain have U-shaped cross sections and display a convex bathymetric profile along their floors (Figure 4 – inset a).

The rate at which a longitudinal profile becomes flatter downstream is known as its concavity (Covault et al., 2011). Convex profiles are often seen in tectonically active areas where changes in the equilibrium of submarine canyons influence their drainage system dynamics (O'Grady et al., 2000; Seybold et al., 2021; Soutter et al., 2021). Ridges in the canyons' downstream portions may be evidence that the active deformation front has contributed to the deformation of the canyons (Figure 3a) and likely influenced the development of the drainage system. (Figure 4; inset a).

The activity along the deformation front significantly influences the morphology of submarine slopes and affects the ability of canyons to reach equilibrium (Pettinga and Jobe, 2021). This is revealed by the decreased concavity of submarine canyons formed in forearc basins, which commonly undergo active seafloor deformation through folding, faulting, or accretionary prism formation (Pirmez et al., 2000; Soutter et al., 2021). The Sinu accretionary prism, Colombia (Vinnels et al., 2010), and the Cook Strait, New Zealand (Micallef et al., 2014), are examples of other locations where thrust faulting has modified the profiles of incisional submarine canyons and their channels, causing them to be convex.

The U-shaped canyon axis suggests sediment accumulation, indicating that sediment transport to the deep basin has decreased (Shepard, 1981). Ridges formed by the active deformation front act as a barrier to sediment transport along the canyons to deeper basins. In addition to the fact that the active deformation front reduces the transport capacity of the canyon, there is also the probability that the canyon receives less sediment at its head due to the formation of terraces on the northern wall of the SOFZ fault trace (see Figure 3a and 4, section h-h'). These terraces may result from the deep channel made by the SOFZ, in which bottom current oscillations may have preferentially eroded, as described in the Atlantic margin (Isola et al., 2021). Cumulative vertical displacements from the deepest to the shallower terrace, totaling 225 m, cannot be explained solely by sea level variations (assumed to be around 120 m). Two possibilities can be proposed: one is the uplift associated with the SOFZ, and the second is the erosion caused by the action of deep currents, as described by Hernandez-Molina et al. (2008). The deep SOFZ channel and the uplift of its northern wall are likely obstructing the canyon's sediment source from the coasts, as the sediments are trapped in the deep valley shaped by the SOFZ trace.

5.3 Contrasting Deformation Styles and Distribution of the Morphological Features

This study proposes two distinct morpho-structural domains from east to west (Figure 14). Between these two domains, lies a NNE-SSW trending transition zone within which numerous aftershocks occurred with deep (50 - 130 km) to shallow (5 - 30 km) epicenters following the Mw 5.9 seismic event on October 6, 2018 (Figure 14). This transition zone is marked by a bathymetric low with landslide scars (Figure 3b). It extends across the Hispaniola margin and the deformation front and runs along the eastern edge of the Great Inagua Bank, which behaves as a rigid stable block that reduces and reverses the Northern Haitian sub-basin slope from the Northern Hispaniola Prism and deformation front (Figure 4 –section D-D', and 2b). It also marks the transition from the narrower prism and more linear deformation front of the Western domain to the wider prism and sinuous deformation front of the Eastern domain (Figure 14). Rodriguez-Zurrunero et al. (2020) proposed several tectonic domains based on an integrated structural, morphological, seismotectonic, and kinematic study, such as Northern Cuba collision, strike-slip and Oblique underthrusting domains (Figure 14). We propose that

the Western and Eastern domains correspond to the Haitian Strike-slip and the Dominican Republic Oblique Underthrusting domains, respectively (Figure 14). The difference in the trend of the SOFZ segments S2 and S3 from SOFZ segments S4 and S5 (Figures 2 and 14), the variation in sediment flux intensity, and the initiation of the indentation of the Great Inagua Bank into the margin could explain the different morphologic and tectonic patterns in the two domains. The nature of the North American plate could play a role in the morpho-structural variation of these two domains. A continental nature could be proposed for the Western domain with the presence of tilted blocks to the north of Cuba on which the Bahamas Carbonate Banks are located (Oliveira de Sá et al., 2024). While an oceanic nature could be proposed for the Eastern domain, which would allow the plate to undergo subduction, as has been suggested by Calais et al. (2023) (Figure 14).

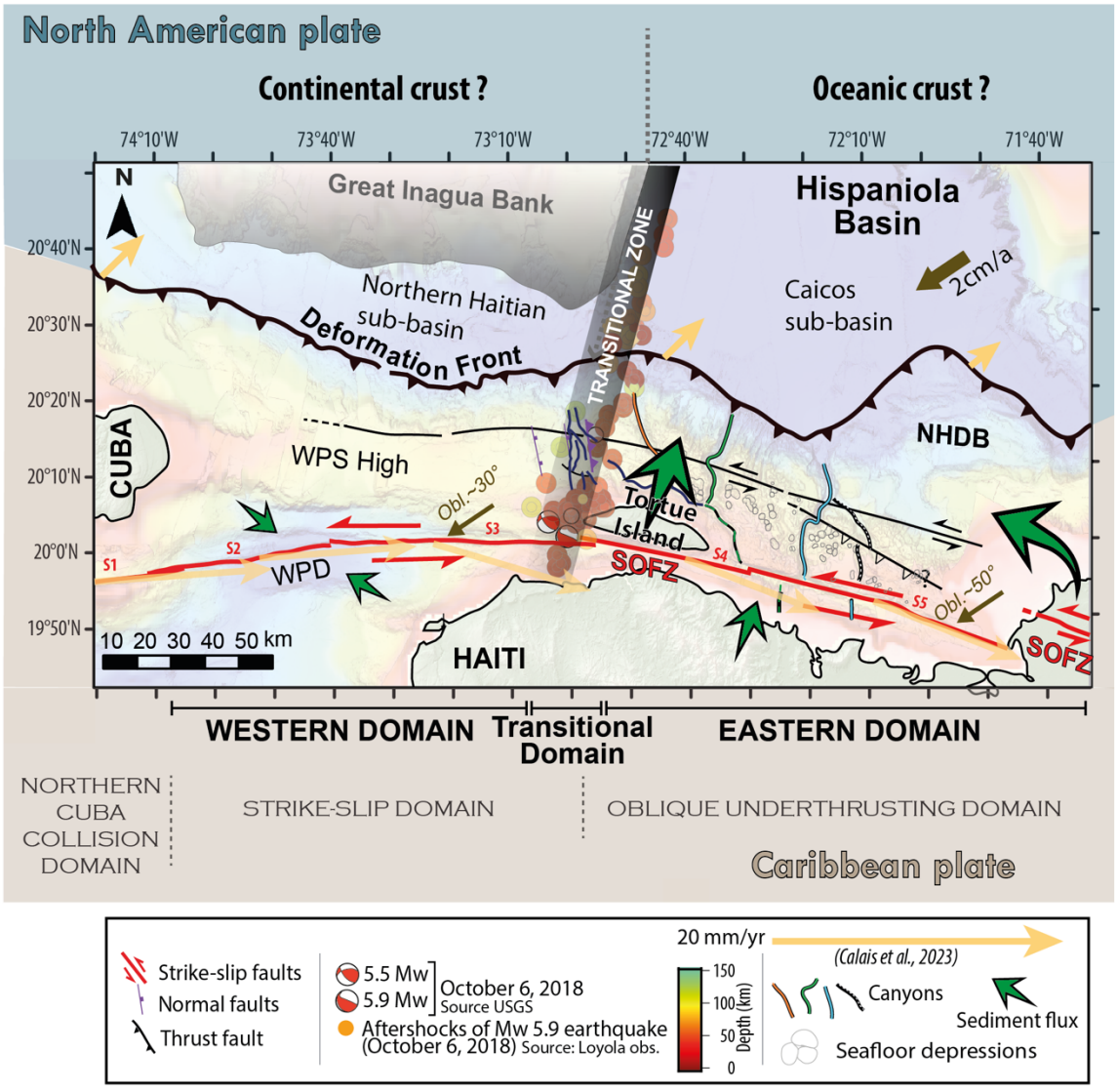

Figure 14: Schematic map showing the different characteristics of the Western and Eastern domains and the proposed nature of the North American Plate. The boundaries of the tectonic domains (collision, strike-slip, oblique underthrusting), derived from Rodriguez-Zurrunero et al. (2020), are in agreement with the findings of our study. The kinematic vectors in yellow are derived from the block model proposed by Calais et al. (2023). Epicenter depth and location information of earthquakes from Loyola observatory (https://www.fdsn.org). WPS: Windward Passage Sill; WPD: Windward Passage Deep.

In the Eastern domain, large-scale sediment flow with the deposition of a fluid-rich layer at the base of U4 is the probable origin of instability caused subsequent differential deformation of this unit. This deformation of U4 created irregularities on the seafloor, which may be indirectly responsible for some of the seafloor depressions but is not the direct cause. Sedimentary and erosional processes induced by bottom currents combined with the irregular bathymetry of the seafloor are more probable causes of the majority of the seafloor depressions. The more detailed characterization of the recent sedimentary deposits of this margin and the possible sedimentary processes causing these depressions on the seafloor on the northern coast of Haiti are discussed in a dedicated paper by Oliveira de Sá et al. (2025).

The major canyons probably began their incision in continuity with terrestrial rivers. In this case, the presence of a significantly developed canyon system exclusively located in the Eastern domain of the study area is again likely due to its direct proximity to the north coast of Hispaniola. In contrast, the Windward Passage Sill in the Western domain is surrounded on each side by two deep basins, at least during the deposition of U4.

These canyons have been affected by the regional transpressive collision (Figure 14). The establishment of strike-slip faults began to affect the course of the canyons' incision, and activity on the deformation front resulted in a progressive uplift of this margin, altering the equilibrium profile of the canyons (Figure 4 – inset a). Therefore, the propagation of the SOFZ-segments at the canyon heads and the activity at the deformation front appear to have rendered these canyons inactive, as indicated by their convex profiles (Figure 4).

5.4 Evolution of the Deformation along the Northern Hispaniola Margin

5.4.1 From Oligocene to Early Pliocene (Unit 1 to 3; Uc4; onset of U4a)

In the Late Oligocene (~20 Ma), the northern Caribbean Plate boundary shifted south of Cuba towards the Oriente Fault Zone (OFZ) (Figure 1b – step a), separating Cuba from Hispaniola, which had until then formed a single block (Calais and Mercier De Lépinay, 1991, 1995; Pindell and Draper, 1991). This tectonic shift resulted in the attachment of the Cuban block to the North American Plate (Calais and Mercier de Lépinay, 1992; Mann et al., 1995; Calais and Mercier de Lépinay, 1995; Leroy et al., 2000; Rojas-Agramonte et al., 2008; Wessels, 2019; Oliveira de Sá et al., 2021).

The OFZ propagated eastward from the Oligocene to the early Miocene (Figure 1b – step a). During this time, the OFZ was the western continuation of the Septentrional Fault in Northern Hispaniola (SF in Figure 1b – step a) (Dolan et al., 1998; Draper et al., 1994; Erikson et al., 1998; Oliveira de Sá et al., 2021).

The Oligocene-Early Middle Miocene rocks of the Septentrional Cordillera exhibit NE-SW shortening and NW-SE trending folds (Erikson et al., 1998; Escuder-Viruete et al 2020). These characteristics point to a middle Miocene deformation episode, which aligns with the formation of a restraining bend along the northern Hispaniola margin (Figure 1b – step a) (De Zoeten and Mann 1991). The ongoing deformation within this restraining bend potentially triggered the folding of the sedimentary units in the study area before Uc4a (Figure 1b – step a). Oliveira de Sá et al. (2021) proposed that thrust faults formed in the Windward Passage during this restraining bend activity in the Early-Middle Miocene (Figures 1b – step a and 8b). Ongoing compression in the Northern Haitian margin folded U1 and created space to accommodate U3 deposition (Figure 5) (Calais and Mercier De Lépinay, 1995; Oliveira de Sá et al., 2021).

This event led to the regional uplift and exposure of the future Septentrional Cordillera, as evidenced by an extensive angular unconformity observed on a regional scale between middle and upper Miocene up to Pliocene (de Zoeten and Mann, 1991; Erikson et al., 1998; Pindell and Draper, 1991; McNeill et al 2013). The erosive phase induced by the subaerial

exposure is expressed on our seismic profiles by Uc4 (Figures 5 to 11). Consequently, erosion would have started during the Middle Miocene, earlier than the Mid-Pliocene age proposed by Oliveira de Sá et al. (2021).

As restraining bends do not efficiently accommodate the regional transcurrent shear of the fault system (Cooke et al., 2013), new strands of the OFZ evolved toward the east to accommodate part of the ongoing strike-slip (red line, Figure 1b – inset b). The initiation of the lateral fault that displaces the canyon's paths and also the initiation of the Camu fault (CF) (Late Miocene, Early Pliocene) and other fault segments in the Septentrional Cordillera are probably related to this process (Figure 1b – steps b and c). The successive southward jumps of these fault segments result in formation of the SFZ and finally the SOFZ when the east and west fault systems joined (Figure 1b – step d).

The Middle Miocene formations observed in the Septentrional Cordillera are characterized by a deepening succession evolution from mixed sandstones and conglomerates in its base (Cercado Formation) to siltstone/mudstone accumulations at its middle (Gurabo Formation) and calcareous siltstone at its top (Mao Formation) corresponding to the Yaque Group (Erikson et al., 1998) (Figure 1b – steps b and c). These formations are interrupted by a relatively thin interval of conglomerate and sandstone beds interpreted as sediment gravity flows. Based on these observations, Erikson (1998) suggested a period of subsidence in which these deep-water formations were deposited following the uplift period recorded during the Middle Miocene (Figure 1b – steps a-b). The detrital middle Miocene sediments were mainly derived from the south, probably from the Central Cordillera, with only brief contributions from the Septentrional Cordillera. Erikson (1998) concluded that from the late Miocene time to the Early Pliocene, the ongoing SFZ (North Hispaniola area, Figure 1b – steps b-c) was the locus of significant strike-slip motion but only minor vertical movement.

The inferred offshore fluid-rich layer in the basal part of U4a is probably the equivalent in age of this coarser Middle Miocene formations on land (Figure 1b – step b). The sand was probably transported during turbidite flows and deposited in a channel-levee system (as depicted by its double-wedge shape lateral to the canyons axis, Figure 9).

5.4.2 Pliocene (Further U4a)

The Pliocene's oblique collision of Hispaniola with the Bahama Banks slowed Hispaniola's eastward movement compared to the North American Plate (Calais et al., 2016). Transpressive deformation, caused by oblique collision, likely led to the formation of the SOFZ, the growth of the deformation front, and the uplift of the Septentrional Cordillera (Sept. C. in Figure 1a and b – step c) (Calais et al., 2016; Escuder-Viruete and Pérez, 2020).

The tectonic activity in the Pliocene significantly affected the northern Haitian margin. With the rise of the Septentrional Cordillera, the sedimentary deposits in the study area became more proximal. In this context of regional uplift, we can infer that the canyons system in the study area developed and increased their incision during the Pliocene due to the upstream uplift gradient.

This upstream uplift produces more concave-shape canyons (Soutter et al., 2021). The canyons in the study area were probably very erosive during the Pliocene, transporting the sediment from the Septentrional Cordillera to the deep Hispaniola basin (Caicos sub-basin). However, it is known that in convergent margins, upstream uplift is counterbalanced by the downstream uplift generated by the activity of thrust fault in the deformation front (Soutter et al., 2021). This process would explain the current convex shape of canyons in the Eastern domain (Figure 4).

The activity of the deformation front during the Pliocene triggered the uplift of the northern Haitian margin. In the Western domain, the proximity to the Great Inagua Bank prevents the deformation front from propagating northward (Figure 2). This is why the thrust

faults are more closely spaced in the Western domain, and the prism is shorter and steeper (Figure 6). The linear scarps that form the narrow E-W-oriented channel in the Northern Haitian sub-basin between the WPS and the Great Inagua Bank (Figure 3b) show that this oblique collision is the controlling factor of the submarine morphology in the Western domain. The scarps along the entire seafloor of the Windward Passage and the presence of the WPS high are also linked to active tectonics (Figures 2b, 3b, and 7). As the Eastern domain faces the vast Caicos sub-basin, the deformation front can propagate northward, giving rise to the imbricating anticlinal ridges system of the lower prism with the establishment of well-spaced thrust faults (Figure 13) and well-defined ridges on the seafloor (Figures 2b, 3a and 13). The distinct nature of the crust of the Northern American plate on either side of the transitional zone could be invoked for the distinct morpho-structural features observed in the Eastern and Western domains.

5.4.3 From Pliocene to present-day (U4b)

During the Pliocene collision, the major strike-slip motion shifted south to its present location in the Dominican Republic (Calais et al., 2016). (Figure 1 – step d). At the same time, in the Eastern domain, the initiation and/or reactivation of strike-slip faults begins, as well as compression, offsetting the canyons' course. The segments of the SOFZ present on land in the Dominican Republic appear to be the eastward extension of the fault segments that offset the canyons (Figures 1a and 3a). These segments were likely formed at the same time as the propagation of fault segments of the OFZ from the Windward Passage Basin towards the east, offshore of Haiti (Figure 1b – step c).

Progressively, the OFZ splayed eastward, running across the WPD and into northern Hispaniola to form the SOFZ (Figure 1b – steps c-d; Calais and Mercier de Lépinay, 1995; Leroy et al., 2015). Thus, the SOFZ formed in the Late Pliocene when segment 5 started offshore Haiti (Figure 1b – step d). The emplacement of the SOFZ established the current Northern Caribbean Plate boundary and incorporated part of northern Hispaniola into the North American Plate, detaching the canyons in the study area from their continental sediment inputs (Calais et al., 2016; Erikson et al., 1998; Escuder-Viruete and Pérez, 2020; Oliveira de Sá et al 2021).

Despite decreased compressional tectonic activity after the Pliocene, there is evidence of persistent vertical movements in the region (Oliveira de Sá et al., 2021) in the form of Quaternary terraces along the northwestern coastlines of Hispaniola, Tortue Island, and Cuba (Figures 3b and 6) (Authemayou et al., 2023; Calais and Mercier De Lépinay, 1992; Sorel et al., 1991). Reverse faults in the elevated WPS also suggest that significant vertical movement could influence the northern Haitian margin (Figures 2b, 3b, and 7).

5.5 Deformation Front from West to East

Our findings show that the compressive component of deformation along the Northern Boundary of the Caribbean Plate is still active. And, although Cuba remains relatively well attached to the North American Plate at present, some reverse faults near the north coast of the eastern Cuba block are deforming recent seismic units (Oliveira de Sà et al. 2024;), suggesting localized tectonic activity there. This interpretation is reinforced by the recent occurrence of earthquakes along the North Cuban Fault (Figure 15a) (Calais et al., 2023). This major structure is the focus of a study by Oliveira de Sá et al. (2024) and appears to be active along the eastern Cuba block as far as 77°W (Figure 15).

In the Eastern domain, compressive deformation is concentrated in the North Hispaniola Prism. The extent of the deformation front is greater here than in the front of the Great Inagua Bank

block, and thrust faults imbricate the thicker Caicos sub-basin infill. Several questions arise from our observations. Is there a subducted lithospheric slab beneath the island of Hispaniola (Figure 15)? Although such a slab has been documented to the east of Hispaniola, there is no evidence of it in the Western domain (e.g., Zurrunero et al 2020; Calais et al 2023). If such a slab exists, would it be a relic of the proto-Caribbean slab or oceanic lithosphere of the North American Plate? The hypothesis that such a slab would consist of the central Atlantic oceanic lithosphere of the North American Plate seems the most likely. We propose that a predominantly NNE-SSW trending structure could form in the Caicos sub-basin near the deformation front, separating the mid-Atlantic oceanic lithosphere from the thinned continental lithosphere further north, on which the Bahamas Banks and the Great Inagua Banks lie (Figure 15). The Continental Ocean Boundary proposed by Shipper and Mann (2024) indicates a difference in crustal thickness in the central part of Cuba, which lies further west than our proposition. However, the transition from continental to oceanic crust may be more diffuse than suggested. Moreover, our transition occurs at the eastern edge of their suggested 150 Ma hotspot area. Although we do not observe any volcanism in our seismic data, the differences in deformation, sedimentation, and seismicity (Figure 16), we observe may be due to variations in thickness outlined by Shipper and Mann (2024).

In the Western domain, the Northern Hispaniola Prism exhibits shortening, while the Northern Haitian sub-basin displays a reverse slope inclined towards the south (Figure 4). We interpreted this as signs of an initiation of a collision zone between the thick continental lithosphere of the Bahamas Carbonate Province on the North American Plate and the Caribbean lithosphere of the Western domain (Figure 15). Indeed, in this area, all the ancient oceanic crust of the proto-Caribbean appears to have been subducted (Figure 15b) (Oliveira de Sá et al., 2024; Neill et al., 2014).

In view of the marked difference in nature of the deformation of the Western and Eastern domains, we propose that they are comprised of two distinct types of lithosphere: continental in the Western domain and oceanic in the Eastern domain. If this is the case, it raises the question of a potential accommodation zone between distinct types of lithosphere of the two domains. Could this accommodation be superficial (crustal) or deeper (lithospheric), such as a slab tear?

The epicenters of aftershocks related to the seismic event on October 6th, 2018, both near the surface (0-30 km) and at depth (40-130 km), are situated in alignment with the proposed NE-SW transition zone west of Tortue Island (Figure 16). Additionally, deeper seismic activity was recorded both before and after the main events (Figures 16a and 16c). We have identified a bathymetric depression associated with faults in this same zone. These observations support the notion of deformation accommodation in this zone, at least on a crustal scale, within the Caribbean Plate. We propose that a significant feature at depth, such as a slab tear in the transition zone (Figures 14 and 15), delineates the edge of an intermediate oceanic continental subducting plate (Figures 14 and 16). To the east of our study area, oceanic lithosphere is being subducted near the Island of Puerto Rico. We propose that this subducting oceanic lithosphere near Puerto Rico transitions to an intermediate oceanic-continental type lithosphere of the study area's Eastern domain. This intermediate lithosphere may be resistant to subduction and may be underthrusting the North American Plate.

A slab tear is proposed to accommodate the change in the type of lithosphere undergoing subduction between the Puerto Rico domain (oceanic lithosphere) and the Eastern domain of our study area, where a transitional lithosphere seems to be more resistant to subduction. Then, a transition zone is proposed to mark the transition from the subduction of an intermediate lithosphere to the purely collisional domain towards Cuba between the two continental lithospheres of the Bahamas and Cuba. The trend of this transition could be related to the previous continental rifted axis.

The tectonic domains defined by Rodriguez-Zurrunero (CD, SSD, OUD, OSD in Figure 15) and the block model vectors of Calais et al. (2023) appear to coincide with the morpho-structural domains we have identified (Figures 14 and 15). The transition zone marks a change in tectonic regime, moving from a collision zone where the underthrusting of the Bahamas platform under the Caribbean plate is blocked to a zone where the underthrusting is still effective.

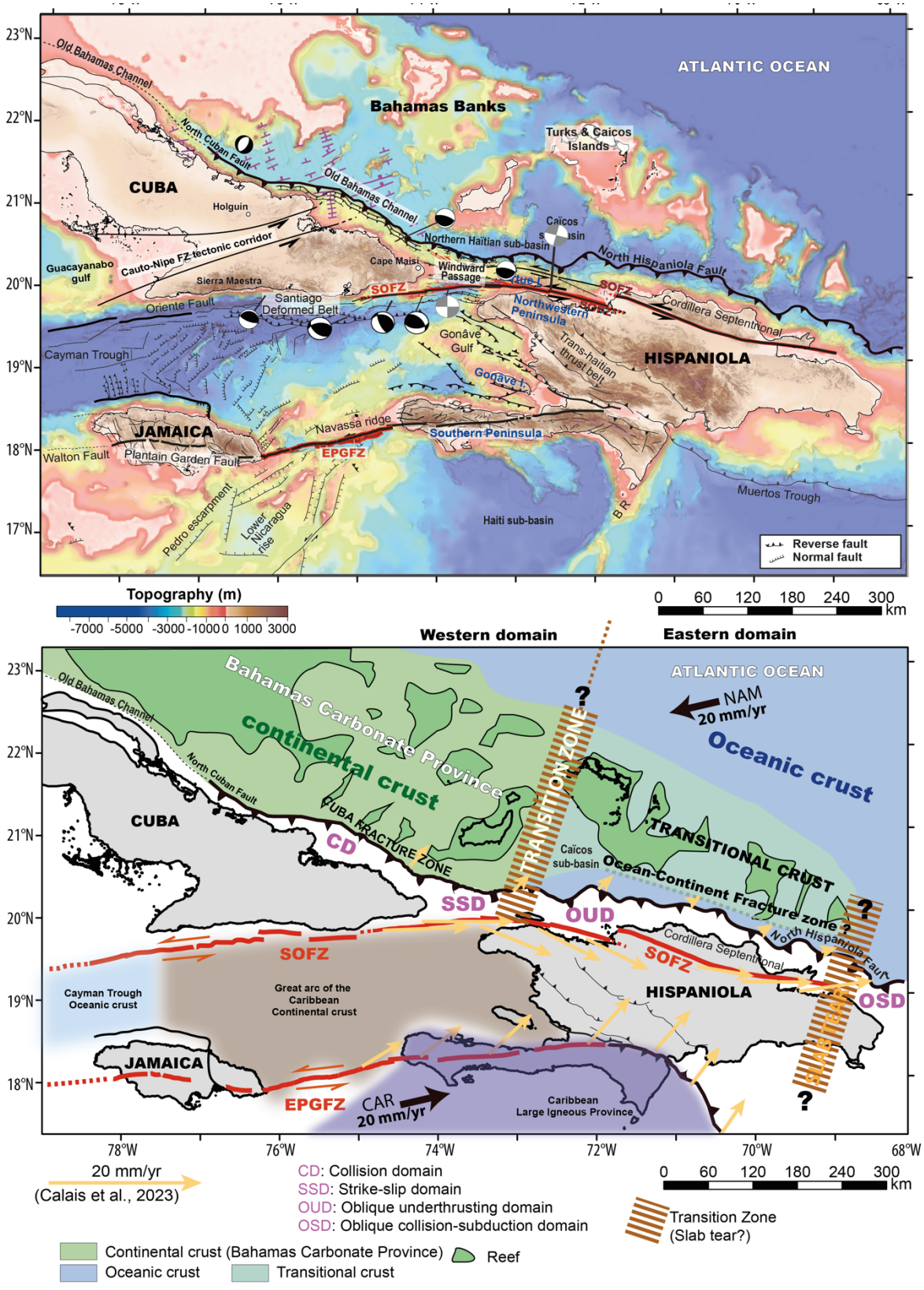

Figure 15: Top: Bathymetric and topographic map of the study area with the main structural features and focal mechanisms (Source: Calais et al., 2023) NHF: North Hispaniola fault; SOFZ: Septentrional-Oriente fault zone; EPGFZ: Enriquillo-Plantain Garden Fault Zone. Bottom: Summary sketch illustrating various hypothetical crustal domains. Kinematic vectors in yellow are taken from the block model proposed by Calais et al (2023). The tectonic

domains are those proposed by Rodriguez-Zurrunero et al. (2020) and in agreement with Sun et al. (2021) for the east. NAM: North American plate; CAR: Caribbean plate.

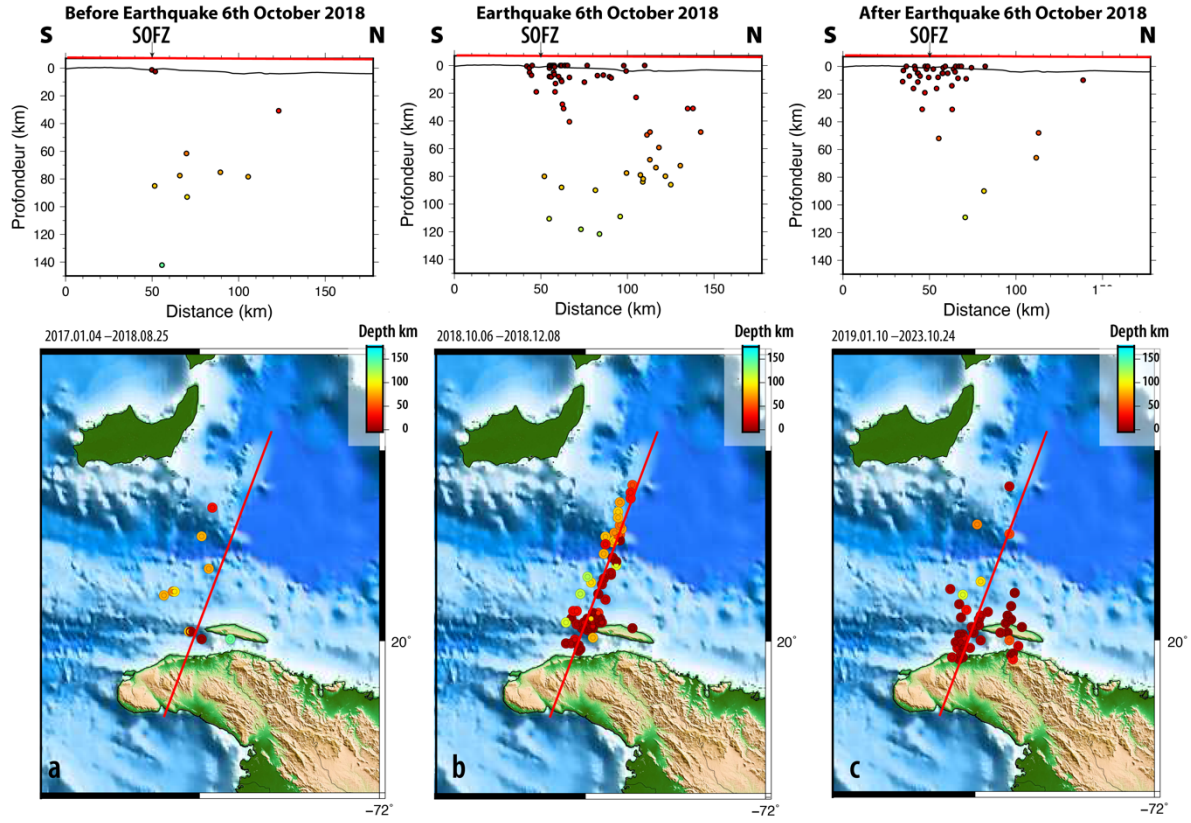

Figure 16: Seismic events from the catalog of Loyola Observatory in the Northern Haitian margin. The three panels show the seismicity before, during and after the main earthquake of 6th October 2018 (Data from the Observatorio Sismologico del Politecnico Loyola, San Cristobal, Dominican Republic. https://ospl.ipl.edu.do/).

6. Conclusion

The tectonic and sedimentary evolution of the Northern Haitian Margin, occurring from the Oligocene to the Late Pliocene, exhibits complex dynamics related to a series of interconnected geological events. The Late Oligocene witnessed a shift in the northern Caribbean Plate boundary, separating Hispaniola from the Cuban block attached to the North American Plate. This tectonic change initiated the Oriente Fault Zone (OFZ), which propagated eastward from the Oligocene to the early Miocene (north of Hispaniola). A middle Miocene restraining bend caused the folding and emersion of pre-Miocene sedimentary formations. This deformation pattern, characterized by a significant unconformity (Uc 4) during the final erosion phase, was observed throughout the study area. The area was submerged again from the late Miocene to early Pliocene due to subsidence. Variations between the Eastern and Western domains arise from different sediment flux and deformation patterns. In the Eastern Domain, a mass transport deposit likely causes differential compaction, leading to post-depositional remobilisation. This results in the wave-like pattern in the Eastern domain, unlike the planar stratigraphy of the Western domain. The ancient MTD constituted an irregular surface affecting current sedimentation and erosion processes on the seafloor. In the late Pliocene, the collision between Hispaniola and the Carbonate Bahamas caused compressive deformation. This deformation initiated the deformation front, evolved the Septentrional Fault Zone, and uplifted the Septentrional Cordillera. Submarine canyons also underwent morphological changes due to tectonism and sediment transport. During this period, the OFZ shifted southward, correlating with new strike-slip faults in the Eastern domain that disrupted the canyons' trajectory. The variations in fault density, cumulative displacement along strike-slip faults, the morphology of the Northern Hispaniola insular slope (including width and tectonic style), and the tilting of basin surfaces indicate the presence and importance of a transitional lithosphere that accommodates tectonic forces. This is particularly evident through seismic activity aligned with a suggested transition zone within the upper Caribbean Plate. The geological evolution of the northern Haitian margin highlights the complex interactions among tectonic mechanisms, sedimentary processes, and the arrangement of geomorphological features. Since the emergence of the OFZ in the Late Oligocene and the establishment of the SOFZ in the Late Pliocene, the intricate relationships among these elements have significantly shaped the seafloor of the Northern Haitian area.

Declaration of competing interest

The authors declare that they have no known competing financial interests or personal relationships that could have appeared to influence the work reported in this paper.

Data availability Data will be made available on request.

Acknowledgements

This paper is a contribution of the HAITI-Fault and HAITI-SIS teams. The processing and the detailed analysis of these geophysical and geological data are mainly carried out in the framework of the HAITI-Fault project at ISTeP. The HAITI-SIS oceanographic campaigns were mainly funded by the Flotte Océanographique Française (French Oceanographic Fleet) and the ISTeP. Authors thank the Complutense University for sharing the NORCARIBE (2013) multibeam bathymetric data. The interpretation was partially funded by project PID2022-138360NB-I00 and ANR JCJC ANR-17-03CE-0004. We thank IHS Kingdom Suites for

allowing us to use the software at ISTeP. We thank Captain P. Moimeaux, the crews, and the technicians from the R/V L'Atalante? (FOF by IFREMER/GENAVIR). The Sorbonne Université funded Oliveira de Sà's Ph.D. We also gratefully acknowledge Christine Authemayou and an anonymous reviewer for their helpful comments.

References

Authemayou, C., Nuñez, A., Pedoja, K., Peñalver, L., Chauveau, D., Dunán-Avila, P., Martin-Izquierdo, D., de Gelder, G., Husson, L., Castellanos Abella, E., Benítez Frómeta, P. de J., & Pastier, A.-M. (2023). Oblique Collision of the Bahamas Platform at the Northern Boundary of the Caribbean Plate Recorded by the Late Cenozoic Coastal Terraces of SE Cuba. *Tectonics*, *42*(8), e2023TC007806. https://doi.org/10.1029/2023TC007806

Benford, B., DeMets, C., & leroys, É. (2012). GPS estimates of microplate motions, northern Caribbean: Evidence for a Hispaniola microplate and implications for earthquake hazard. *Geophysical Journal International*, *191*(2), 481-490. https://doi.org/10.1111/j.1365-246X.2012.05662.x

Calais, É., Freed, A., Mattioli, G., Amelung, F., Jónsson, S., Jansma, P., Hong, S.-H., Dixon, T., Prépetit, C., & Momplaisir, R. (2010). Transpressional rupture of an unmapped fault during the 2010 Haiti earthquake. *Nature Geoscience*, *3*(11), Article 11. https://doi.org/10.1038/ngeo992

Calais, E., Gonzales, O., Arango-Arias, E. D., Moreno, B., Clares, R. P., Cutie, M., Diez, E., Montenegro, C., Roche, E. R., Garcia, J., Castellanos, E., & Symithe, S. (2023). *Current Deformation Along the Northern Caribbean Plate Boundary from Gnss Measurements in Cuba* (SSRN Scholarly Paper 4537779). https://doi.org/10.2139/ssrn.4537779

Calais, E., & Mercier De Lépinay, B. (1991). From transtension to transpression along the northern Caribbean plate boundary off Cuba: Implications for the Recent motion of the Caribbean plate. *Tectonophysics*, *186*(3), 329-350. https://doi.org/10.1016/0040-1951(91)90367-2

Calais, E., & Mercier De Lépinay, B. (1992). La limite de plaques décrochante Nord Caraïbe en Hispaniola : Évolution paléogéographique et structurale cénozoïque. *Bull. Soc. géol*, *3*(163), 309-324.

Calais, E., & Mercier De Lépinay, B. (1995). Strike-slip tectonic processes in the northern Caribbean between Cuba and Hispaniola (Windward Passage). *Marine Geophysical Researches*, *17*(1), 63-95. https://doi.org/10.1007/BF01268051

Calais, E., Symithe, S., Mercier de Lépinay, B., & Prépetit, C. (2016). Plate boundary segmentation in the northeastern Caribbean from geodetic measurements and Neogene geological observations. *Comptes Rendus Geoscience*, *348*(1), 42-51. https://doi.org/10.1016/j.crte.2015.10.007

Conrad, E.M., Faccenna, C., Holt, A.F., Becker, T.W., 2024. Tectonic Reorganization of the Caribbean Plate System in the Paleogene Driven by Farallon Slab Anchoring. Geochem Geophys Geosyst 25, e2024GC011499. https://doi.org/10.1029/2024GC011499

Cooke, M. L., Schottenfeld, M. T., & Buchanan, S. W. (2013). Evolution of fault efficiency at restraining bends within wet kaolin analog experiments. Journal of Structural Geology, 51, 180-192. https://doi.org/10.1016/j.jsg.2013.01.010

Cotilla-Rodríguez, M. O. (2021). Historia de la sismicidad del segmento Islas Caimán-Cabo Cruz (Cuba), en el marco de la zona de entre placas Norteamérica-Caribe. *Revista Tierra*, *1*(1), Article 1. https://revistatierra.unan.edu.ni/index.php/revista_tierra/article/view/25

Covault, J.A., Fildani, A., Romans, B.W., McHargue, T., 2011. The natural range of submarine canyon-and-channel longitudinal profiles. Geosphere 7, 313–332. https://doi.org/10.1130/GES00610.1

Davies, R. J. (2005). Differential compaction and subsidence in sedimentary basins due to silica diagenesis: A case study. *GSA Bulletin*, *117*(9-10), 1146-1155. https://doi.org/10.1130/B25769.1

Davies, R. J., Huuse, M., Hirst, P., Cartwright, J., & Yang, Y. (2006). Giant clastic intrusions primed by silica diagenesis. *Geology*, *34*(11), 917-920. https://doi.org/10.1130/G22937A.1

de Zoeten, R., & Mann, P. (1991). Structural geology and Cenozoic tectonic history of the central Cordillera Septentrional, Dominican Republic. In *Geological Society of America Special Papers* (Vol. 262, p. 265-280). Geological Society of America. https://doi.org/10.1130/SPE262-p265

de Zoeten, R., & Mann, P. (1999). Chapter 11 Cenozoic el Mamey group of northern Hispaniola: A sedimentary record of subduction, collisional and strike-slip events within the north America-Caribbean plate boundary zone. In P. Mann (Éd.), *Sedimentary Basins of the World* (Vol. 4, p. 247-286). Elsevier. https://doi.org/10.1016/S1874-5997(99)80045-8

Dillon, W. P., Austin, J. A., Scanlon, K. M., Terence Edgar, N., & Parson, L. M. (1992). Accretionary margin of north-western Hispaniola: Morphology, structure and development of part of the northern Caribbean plate boundary. *Marine and Petroleum Geology*, *9*(1), 70-88. https://doi.org/10.1016/0264-8172(92)90005-Y

Dillon, W. P., Edgar, N. T., Scanlon, K. M., & Coleman, D. F. (1996). *A review of the tectonic problems of the strike-slip northern boundary of the Caribbean Plate and examination by GLORIA: Chapter 9*. 135-168.

Dolan, J. F., Mullins, H. T., & Wald, D. J. (1998). Active tectonics of the north-central Caribbean: Oblique collision, strain partitioning, and opposing subducted slabs. In J. F. Dolan & P. Mann, *Active Strike-Slip and Collisional Tectonics of the Northern Caribbean Plate Boundary Zone*. Geological Society of America. https://doi.org/10.1130/0-8137-2326-4.1

Draper, G., Mann, P., & Lewis, J. F. (1994). Hispaniola. In S. K. Donovan & T. A. Jackson, *Caribbean Geology: An Introduction. University of the West Indies Publishers Association* (p. 129-150).

Emery, K. O. (1980). Continental margins: Classification and petroleum prospects. *Am. Assoc. Pet. Geol. Bull.; (United States)*, *64:3*. https://www.osti.gov/biblio/7048945

Erikson, J., Pindell, J., Karner, G., Sonder, L., Fuller, E., & Dent, L. (1998). Neogene Sedimentation and Tectonics in the Cibao Basin and Northern Hispaniola: An Example of Basin Evolution Near A Strike-Slip-Dominated Plate Boundary. *The Journal of Geology*, *106*. https://doi.org/10.1086/516036

Escuder-Viruete, J., & Pérez, Y. (2020). Neotectonic structures and stress fields associated with oblique collision and forearc sliver formation in northern Hispaniola: Implications for the seismic hazard assessment. *Tectonophysics*, *784*, 228452. https://doi.org/10.1016/j.tecto.2020.228452

Escuder-Viruete, J., Beranoaguirre, A., Valverde-Vaquero, P., McDermott, F., 2020. Quaternary deformation and uplift of coral reef terraces produced by oblique subduction and underthrusting of the Bahama Platform below the northern Hispaniola forearc. Tectonophysics 796, 228631. https://doi.org/10.1016/j.tecto.2020.228631

Etienne, S., Le Roy, P., Tournadour, E., Roest, W. R., Jorry, S., Collot, J., Patriat, M., Largeau, M. A., Roger, J., Clerc, C., Dechnick, B., Sanborn, K. L., Lepareur, F., Horowitz, J., Webster, J. M., & Gaillot, A. (2021). Large-scale margin collapses along a partly

drowned, isolated carbonate platform (Lansdowne Bank, SW Pacific Ocean). *Marine Geology*, *436*, 106477. https://doi.org/10.1016/j.margeo.2021.106477

Gay, A., Lopez, M., Cochonat, P., & Sermondadaz, G. (2004). Polygonal faults-furrows system related to early stages of compaction – upper Miocene to recent sediments of the Lower Congo Basin. *Basin Research*, *16*(1), 101-116. https://doi.org/10.1111/j.1365-2117.2003.00224.x

Goreau, P. D. (1981). *The tectonic evolution of the North Central Caribbean plate margin*. Massachusetts Institute of Technology, Dept. of Earth and Planetary Sciences.

Harris, P. T., & Whiteway, T. (2011). Global distribution of large submarine canyons: Geomorphic differences between active and passive continental margins. *Marine Geology*, *285*(1-4), 69-86.

Herbert, T. D. (1993). Differential compaction in lithified deep-sea sediments is not evidence for "diagenetic unmixing". *Sedimentary Geology*, *84*(1), 115-122. https://doi.org/10.1016/0037-0738(93)90049-B

F.J. Hernández-Molina, A. Maldonado, D.A.V. Stow, 2008, Chapter 18 Abyssal Plain Contourites, Editor(s): M. Rebesco, A. Camerlenghi, Developments in Sedimentology, Elsevier, V. 60, 345-378.

Hurst, A., Cartwright, J., Huuse, M., Jonk, R., Schwab, A., Duranti, D., & Cronin, B. (2003). Significance of large-scale sand injectites as long-term fluid conduits: Evidence from seismic data. *Geofluids*, *3*(4), 263-274. https://doi.org/10.1046/j.1468-8123.2003.00066.x

Huuse, M., Cartwright, J., Hurst, A., & Steinsland, N. (2007). Seismic characterization of large-scale sandstone intrusions. *Sand Injectites: Implications for Hydrocarbon Exploration and Production*, *87*, 21-35.

Isola, J.I., Bravo, M.E., Bozzano, G., Palma, F.I., Ormazabal, J.P., Principi, S., Spoltore, D., Martin, R., Esteban, F.D., Tassone, A.A., 2021. The Late-Quaternary deposits of the Piedra Buena Terrace (Patagonian continental slope, SW Atlantic): An example of interaction between bottom currents and seafloor morphology. Marine Geology 435, 106459. https://doi.org/10.1016/j.margeo.2021.106459

Iturralde-Vinent, M. A., García-Casco, A., Rojas-Agramonte, Y., Proenza, J. A., Murphy, J. B., & Stern, R. J. (2016). The geology of Cuba: A brief overview and synthesis. *GSA Today*, 4-10. https://doi.org/10.1130/GSATG296A.1

Jackson, C. (2007). The geometry, distribution, and development of clastic injections in slope systems: Seisimic examples from the Upper Creataceous Kyrre formation, Måløy slope, Norwegian margin. *Sand Injectites: Implications for Hydrocarbon Exploration and Production*, 21-35.

Kane, I. A. (2010). Development and flow structures of sand injectites : The Hind Sandstone Member injectite complex, Carboniferous, UK. *Marine and Petroleum Geology*, *27*(6), 1200-1215. https://doi.org/10.1016/j.marpetgeo.2010.02.009

Kane, I. A., & Hodgson, D. M. (2011). Sedimentological criteria to differentiate submarine channel levee subenvironments: Exhumed examples from the Rosario Fm. (Upper Cretaceous) of Baja California, Mexico, and the Fort Brown Fm. (Permian), Karoo Basin, S. Africa. *Marine and Petroleum Geology*, *28*(3), 807-823. https://doi.org/10.1016/j.marpetgeo.2010.05.009

Lee, S. H., & Chough, S. K. (2001). High-resolution (2–7 kHz) acoustic and geometric characters of submarine creep deposits in the South Korea Plateau, East Sea. *Sedimentology*, *48*(3), 629-644. https://doi.org/10.1046/j.1365-3091.2001.00383.x

Leroy, S. (2012). *HAITI-SIS cruise,L'Atalante R/V*. https://doi.org/10.17600/12010070

Leroy, S., & Ellouz-Zimmermann, N. (2013). *HAITI-SIS2 cruise, L'Atalante R/V*. https://doi.org/10.17600/13010080

Leroy, S., Ellouz-Zimmermann, N., Corbeau, J., Rolandone, F., Mercier De Lépinay, B., Meyer, B., Momplaisir, R., Bruña, J.-L. G., Battani, A., Baurion, C., Burov, E., Clouard, V., Deschamps, R., Gorini, C., Hamon, Y., Lafosse, M., Leonel, J., Pourhiet, L. L., Estrada, P. L., … Muñoz, S. (2015). Segmentation and kinematics of the North America-Caribbean plate boundary offshore Hispaniola. *Terra Nova*, *27*(6), 467-478. https://doi.org/10.1111/ter.12181

Leroy, S., Mauffret, A., Patriat, P., & Mercier de Lépinay, B. (2000). An alternative interpretation of the Cayman trough evolution from a reidentification of magnetic anomalies. Geophysical Journal International, 141(3), 539-557. https://doi.org/10.1046/j.1365-246x.2000.00059.x

Li, W., Alves, T. M., Wu, S., Rebesco, M., Zhao, F., Mi, L., & Ma, B. (2016). A giant, submarine creep zone as a precursor of large-scale slope instability offshore the Dongsha Islands (South China Sea). *Earth and Planetary Science Letters*, *451*, 272-284. https://doi.org/10.1016/j.epsl.2016.07.007

Locat, J., & Lee, H. J. (2002). Submarine landslides: Advances and challenges. *Canadian Geotechnical Journal*, *39*(1), 193-212. https://doi.org/10.1139/t01-089

Lonergan, L., Jamin, N. H., Jackson, C. A.-L., & Johnson, H. D. (2013). U-shaped slope gully systems and sediment waves on the passive margin of Gabon (West Africa). *Marine Geology*, *337*, 80-97. https://doi.org/10.1016/j.margeo.2013.02.001

Lonergan, L., Lee, N., Johnson, H. D., Cartwright, J. A., & Jolly, R. J. H. (2000). Remoblization and Injection in Deepwater Depositional Systems: Implications for Reservoir Architecture and Prediction. In P. Weimer (Éd.), *Deep-Water Reservoirs of the World* (Vol. 20, p. 0). SEPM Society for Sedimentary Geology. https://doi.org/10.5724/gcs.00.15.0515

Ma, H.-X., Fan, G.-Z., Shao, D.-L., Ding, L.-B., Sun, H., Zhang, Y., Zhang, Y.-G., & Cronin, B. (2020). Deep-water depositional architecture and sedimentary evolution in the Rakhine Basin, northeast Bay of Bengal. *Petroleum Science*, *17*. https://doi.org/10.1007/s12182-020-00442-0

Mann, P., Calais, É., Ruegg, J.-C., DeMets, C., Jansma, P. E., & Mattioli, G. S. (2002). Oblique collision in the northeastern Caribbean from GPS measurements and geological observations. *Tectonics*, *21*(6), 7-1-7-26. https://doi.org/10.1029/2001TC001304

Mann, P., Taylor, F. W., Edwards, R. L., & Ku, T.-L. (1995). Actively evolving microplate formation by oblique collision and sideways motion along strike-slip faults: An example from the northeastern Caribbean plate margin. *Tectonophysics*, *246*(1), 1-69. https://doi.org/10.1016/0040-1951(94)00268-E

McAdoo, B. G., Pratson, L. F., & Orange, D. L. (2000). Submarine landslide geomorphology, US continental slope. *Marine Geology*, *169*(1), 103-136. https://doi.org/10.1016/S0025-3227(00)00050-5

Micallef, A., Mountjoy, J. J., Barnes, P. M., Canals, M., & Lastras, G. (2014). Geomorphic response of submarine canyons to tectonic activity: Insights from the neill Strait canyon system, New Zealand. *Geosphere*, *10*, 905-929. https://doi.org/10.1130/GES01040.1

Monnier, D., Imbert, P., Gay, A., Mourgues, R., & Lopez, M. (2014). Pliocene sand injectites from a submarine lobe fringe during hydrocarbon migration and salt diapirism: A seismic example from the Lower Congo Basin. *Geofluids*, *14*(1), 1-19. https://doi.org/10.1111/gfl.12057

Neill, I., Kerr, A. C., Chamberlain, K. R., Schmitt, A. K., Urbani, F., Hastie, A. R., Pindell, J. L., Barry, T. L., & Millar, I. L. (2014). Vestiges of the proto-Caribbean seaway: Origin of the San Souci Volcanic Group, Trinidad. Tectonophysics, 626, 170-185. https://doi.org/10.1016/j.tecto.2014.04.019

O'Grady, D. B., Syvitski, J. P. M., Pratson, L. F., & Sarg, J. F. (2000). Categorizing the morphologic variability of siliciclastic passive continental margins. *Geology*, *28*(3), 207-210. https://doi.org/10.1130/0091-7613(2000)28<207:CTMVOS>2.0.CO;2

Oliveira de Sá, A., d'Acremont, E., Leroy, S., & Lafuerza, S. (2021). Polyphase Deformation and Strain Migration on the Septentrional-Oriente Fault Zone in the Windward Passage, Northern Caribbean Plate Boundary. *Tectonics*, *40*(8), e2021TC006802. https://doi.org/10.1029/2021TC006802

Oliveira de Sá, A., Lafuerza, S., Leroy, S., d'Acremont, E., Ducassou, E., Deschamps, R., Zaragosi, S., Fauquembergue, K., Granja-Buña, J. L., Momplaisir, R., & Boisson, D. 2025. Enigmatic deep-water seafloor depressions east of Tortue Island, Northern Haiti margin. *Gcubed accepted*.

Oliveira de Sá, A., Leroy, S., d'Acremont, E., Lafuerza, S., Granja-Bruña, J.-L., Moreno, B., Cabiativa Pico, V., & Letouzey, J., 2024. The Protracted Evolution of a Plate Boundary: Eastern Cuba Block and Old Bahamas Channel. Geochemistry, Geophysics, Geosystems, 25(5), e2023GC011230. https://doi.org/10.1029/2023GC011230

Osborne, M. J., & Swarbrick, R. E. (1998). Mechanisms for Generating Overpressure in Sedimentary Basins: A Reevaluation: Reply1. *AAPG Bulletin*, *82*(12), 2270-2271. https://doi.org/10.1306/00AA7F0E-1730-11D7-8645000102C1865D

Pettinga, L. A., & Jobe, Z. R. (2021). How submarine channels (re)shape continental margins. *Journal of Sedimentary Research*, *90*(11), 1581-1600. https://doi.org/10.2110/jsr.2020.72

Pindell, J. L., & Draper, G. (1991). Stratigraphy and geological history of the Puerto Plata area, northern Dominican Republic. In *Geological Society of America Special Papers* (Vol. 262, p. 97-114). Geological Society of America. https://doi.org/10.1130/SPE262-p97

Pirmez, C., Beaubouef, R. T., Friedmann, S. J., & Mohrig, D. C. (2000). Equilibrium Profile and Baselevel in Submarine Channels: Examples from Late Pleistocene Systems and Implications for the Architecture of Deepwater Reservoirs. In P. Weimer (Éd.), *Deep-Water Reservoirs of the World* (Vol. 20, p. 0). SEPM Society for Sedimentary Geology. https://doi.org/10.5724/gcs.00.15.0782

Rodríguez-Zurrunero, A., Granja-Bruña, J. L., Carbó-Gorosabel, A., Muñoz-Martín, A., Gorosabel-Araus, J. M., Gómez de la Peña, L., Gómez Ballesteros, M., Pazos, A., Catalán, M., Espinosa, S., Druet, M., Llanes, P., & ten Brink, U. (2019). Submarine morpho-structure and active processes along the North American-Caribbean plate boundary (Dominican Republic sector). *Marine Geology*, *407*, 121-147. https://doi.org/10.1016/j.margeo.2018.10.010

Rodríguez-Zurrunero, A., Granja-Bruña, J. L., Muñoz-Martín, A., Leroy, S., ten Brink, U., Gorosabel-Araus, J. M., Gómez de la Peña, L., Druet, M., & Carbó-Gorosabel, A. (2020). Along-strike segmentation in the northern Caribbean plate boundary zone (Hispaniola sector): Tectonic implications. *Tectonophysics*, *776*, 228322. https://doi.org/10.1016/j.tecto.2020.228322

Rojas-Agramonte, Y., Neubauer, F., Garcia-Delgado, D. E., Handler, R., Friedl, G., & Delgado-Damas, R. (2008). Tectonic evolution of the Sierra Maestra Mountains, SE Cuba, during Tertiary times: From arc-continent collision to transform motion. *Journal of South American Earth Sciences*, *26*(2), 125-151. https://doi.org/10.1016/j.jsames.2008.05.005

Safronova, P. A., Andreassen, K., Laberg, J. S., & Vorren, T. O. (2012). Development and post-depositional deformation of a Middle Eocene deep-water sandy depositional system in the Sørvestsnaget Basin, SW Barents Sea. *Marine and Petroleum Geology*, *36*(1), 83-99. https://doi.org/10.1016/j.marpetgeo.2012.06.007

Saller, A., & Dharmasamadhi, I. (2012). Controls on the development of valleys, canyons, and unconfined channel–levee complexes on the Pleistocene Slope of East Kalimantan,

Indonesia. *Marine and Petroleum Geology*, *29*. https://doi.org/10.1016/j.marpetgeo.2011.09.002

Seybold, H., Berghuijs, W. R., Prancevic, J. P., & Kirchner, J. W. (2021). Global dominance of tectonics over climate in shaping river longitudinal profiles. *Nature Geoscience*, *14*(7), Article 7. https://doi.org/10.1038/s41561-021-00720-5

Shepard, F. P. (1965). Types of Submarine Valleys1 : GEOLOGICAL NOTES. *AAPG Bulletin*, *49*(3), 304-310. https://doi.org/10.1306/A663353A-16C0-11D7-8645000102C1865D

Shepard, F. P. (1981). Submarine Canyons: Multiple Causes and Long-Time Persistence. *AAPG Bulletin*, *65*(6), 1062-1077.

Shillington, D. J., Seeber, L., Sorlien, C. C., Steckler, M. S., Kurt, H., Dondurur, D., Çifçi, G., İmren, C., Cormier, M.-H., McHugh, C. M. G., Gürçay, S., Poyraz, D., Okay, S., Atgın, O., & Diebold, J. B. (2012). Evidence for widespread creep on the flanks of the Sea of Marmara transform basin from marine geophysical data. *Geology*, *40*(5), 439-442. https://doi.org/10.1130/G32652.1

Shipper, K., Mann, P., 2024. Crustal Structure, Deformational History, and Tectonic Origin of the Bahamas Carbonate Platform. Geochem Geophys Geosyst 25, e2023GC011300. https://doi.org/10.1029/2023GC011300

Sorel, D., Purser, B. H., & Senatos, H. (1991). Strike-slip tectonic processes in the northern Caribbean between Cuba and Hispaniola (Windward Passage). *Essai de datation des récifs soulevés d'Haiti par la méthode du forcage climatique orbital*, *313*, 1277-1281.

Soutter, E., Kane, I., Hodgson, D., & Flint, S. (2021). The Concavity of Submarine Canyon Longitudinal Profiles. *Journal of Geophysical Research: Earth Surface*, *126*. https://doi.org/10.1029/2021JF006185

Sun, L., Mann, P., Bird, D.E., 2021. Integration of tectonic geomorphology and crustal structure across the active obliquely collisional zone on the island of Hispaniola, northeastern Caribbean. Geological Society, London, Special Publications 504, 379–400. https://doi.org/10.1144/SP504-2019-242

Surlyk, F., Noe-Nygaard, N., & Gjelberg, J. (2007). The Upper Jurassic Hareelv Formation of East Greenland : A Giant Sedimentary Injection Complex. In A. Hurst & J. Cartwright (Éds.), *Sand Injectites : Implications for Hydrocarbon Exploration and Production* (Vol. 87, p. 0). American Association of Petroleum Geologists. https://doi.org/10.1306/1209858M871101

Symithe, S., Calais, É., Chabalier, J. B., Robertson, R., & Higgins, M. (2015). Current block motions and strain accumulation on active faults in the Caribbean. *Journal of Geophysical Research: Solid Earth*, *120*(5), 3748-3774. https://doi.org/10.1002/2014JB011779

Uyeda, S., 1984. Subduction zones: their diversity, mechanism and human impacts. *GeoJournal*, **8**(4), 381–406.

Vinnels, J. S., Butler, R. W. H., McCaffrey, W. D., & Paton, D. A. (2010). Depositional processes across the Sinú Accretionary Prism, offshore Colombia. *Marine and Petroleum Geology*, *27*(4), 794-809. https://doi.org/10.1016/j.marpetgeo.2009.12.008

Wessels, R. J. F. (2019). Chapter 15—Strike-Slip Fault Systems Along the Northern Caribbean Plate Boundary. In J. C. Duarte (Éd.), *Transform Plate Boundaries and Fracture Zones* (p. 375-395). Elsevier. https://doi.org/10.1016/B978-0-12-812064-4.00015-3